國 立 交 通 大 學

機械工程學系

碩 士 論 文

前饋式零相位誤差強健控制器應用於微型化藍光讀寫頭兩段式致動器設計

Dual-Stage Actuator Feed-forward Robust Controller Design with ZPETC Method In Miniaturized Optical Disc Drive

指導教授：鄭泗東　教授

研 究 生：周伯謙

中 華 民 國 九十七 年 七 月

Dual Stage Actuator Feed-forward Robust Controller Design with ZPETC Method In Miniaturized Optical Disc Drive

前饋式零相位誤差強健控制器應用於微型化藍光讀寫頭兩段式致動器設計

研 究 生：周伯謙　　Student : Po-chien Chou

指導教授：鄭泗東教授 Advisor : Dr. Stone Cheng

國 立 交 通 大 學

機械工程學系

碩 士 論 文

Department of Mechanical Engineering,

National Chiao-Tung University,

June 2008

Hsinchu , Taiwan, Republic of China

中 華 民 國 九十七 年 七 月

摘要

有PZT的雙軸控制致動器設計用來提供高速尋軌與聚焦的讀取動作,解決以往微型化讀寫頭(mini-ODD)容易受外在干擾影響而不易快速讀取資料情況,新式的蹺板式雙軸致動器機械上有點對於聚焦能提供更迅速更精確的讀取.主致動器VCM做大範圍的低頻調整移動聚焦尋軌,同時配合PZT精密小範圍高頻的精密調整.遠比傳統單軸VCM來的迅速.在機構的伺服控制方面,期望微型化藍光光學讀寫頭在*10800rpm*高速運轉下,控制系統一方面能達到高速響應,另一方面對於低頻與高頻的干擾能有效排除,現今雙軸伺服控制設計更比起傳統單軸致動器控制器的設計更顯得困難與複雜,再建模基礎下,建立一個有效的強健干擾觀察迴路對致動器做控制,一方面強健傳統PID控制器對於干擾影響的不穩定性,一方面抑制建模過程中系統不確定因素所帶來的影響.對於突發干擾能做有效抑制.解決微型讀寫頭受外在衝擊時對系統讀取碟片所帶來的影響.另外對於PZT壓電效應與碟盤偏心不平整所產生的週期性干擾,以快速零相位誤差控制迴路(ZPET-FF)控制迴路對其做修正,以強健觀察迴路系統抑制突發干擾,以快速零相位誤差控制迴路抑制週期性干擾,在兩者搭配下期望能更快速的達到系統的預估的頻率響應值是本論文的目的

Abstract

A swing-arm/PZT dual-stage actuator is designed to provide high performance solution to realize precise tracking and focusing operation of miniaturized optical disc drive (mini-ODD). Because of its dual-stage mechanical characteristics can perform the focusing action smoother and more precise; the servo system to control such a dual-stage system tends to be more complex than a conventional single-stage ODD system. Based on the modeling results, a robust tracking observer control system with both two degree of freedom control system is proposed. In order to suppress the disturbance quickly, this paper designs the zero phase error tracking controller (ZPETC) plus feed-forward servo loop with the memory of tracking error to satisfy tracking error transient response and improve the sensitive focusing performance of dual-stage miniaturized actuator. The conclusion points out that the proposed robust ZPETC servo system has a precise tracking response and rejects both periodic disturbance and sudden disturbance.

誌謝

感謝指導老師鄭泗東教授這兩年來對我的諄諄教誨與細心指導, 使我不僅再分析邏輯的能力有所提升, 並且完成本篇論文研究. 期間鄭泗東教授的鼎力相助以及支持鼓勵, 使控制實驗可以順利成功, 學生我點滴在心頭, 由衷感激鄭老師的協助與打氣!也感謝林君穎學長與侯冠州學長提供光學頭組裝的設備與量測的空間, 以及對我的關心與鼓勵, 在施錫富教授熱心的指導之下, 使我對於光陸方面的組裝有著顯著的進步, 更謝謝鄭泗東老師與吳炳飛老師使我對控制構思與干擾阻絕研究方向的思考判斷技巧有著顯著的進步, 使的我論文能更臻完整. 此外感謝呂宗熙實驗室學長對於系統健模的幫忙與建議, 讓我在實驗方法與思考方向有更大的突破, 在此也謝謝曹致維, 余偉廷, 郭富存等等好同學提供寶貴建議!同時, 感謝實驗室學長以及學弟的支持與鼓勵, 讓我能夠再碩士求學生涯中留下快樂的回憶

感謝交大電機控制工程研究所, 中興機械工程研究所, 交大光電研究所, 經濟部微型化光學頭計畫, 以及行政院國家科學委員會提供本研究所需的經費, 使得言就可以順利的進行

最後, 僅將本論文獻給一路走來永遠支持我的家人, 謝謝你們對我的關心與照顧, 使我能夠堅持到底地完成學業, 並且打開雙臂迎接嶄新的挑戰

Table of Conents

FIGURE CAPTIONS

INTRODUCTION

1.1 Background

Optical disk drive is one of the most popular systems of information storage. Two promising candidates are near-field recording and holography. Holographic data storage technology provides far-field optical recording and readout. High capacities are obtained by using a very high numerical aperture optical stylus for reading data from and writing data onto the optical disk [4]. In optical holography, data are impressed onto an optical coherent beam using a spatial light modulator. Resulting in very small spot sizes approaching dimensions less than 100 nm, the focusing spot is near to the optical lens, requiring close proximity between the optical head and disk, making removability of the media more difficult. Referring Fig.1, the new servo mechanism of dual stage actuation in the mini-ODD places a small secondary PZT actuator on the optical head. The PZT actuator has been proposed to perform the fine focusing for narrow track pitch, and the Seesaw performs in the role of the major tracking actuator. Optical disk drive is one of the most popular systems of information storage. Two promising candidates are near-field recording and holography. Holographic data storage technology provides far-field optical recording and readout. High capacities are obtained by using a very high numerical aperture optical stylus for reading data from and writing data onto the optical disk [4]. In optical holography, data are impressed onto an optical coherent beam using a spatial light modulator. Resulting in very small spot sizes approaching dimensions less than 100 nm, the focusing spot is near to the optical lens, requiring close proximity between the optical head and disk, making removability of the media more difficult. From the control point view, it cannot be achieved by the current ODDs employing the sole actuator of VCM. The VCM limits the bandwidth extension in the single-stage servo system because of its mechanical resonances and

high frequency uncertainties [3]. As such dual-stage actuation is seen to be the solution for new generation of ODDs. Dual-stage servo control system is proposed to perform the fine positioning for ultra-high focusing speed. Referring Fig. 1.1& Fig1.2, the new servo mechanism of dual stage actuation in the mini-ODD places a small secondary PZT actuator on the optical head. A small secondary PZT actuator has been proposed to perform the fine focusing for ultra-narrow track pitch, and the Seesaw performs in the role of the major tracking actuator.

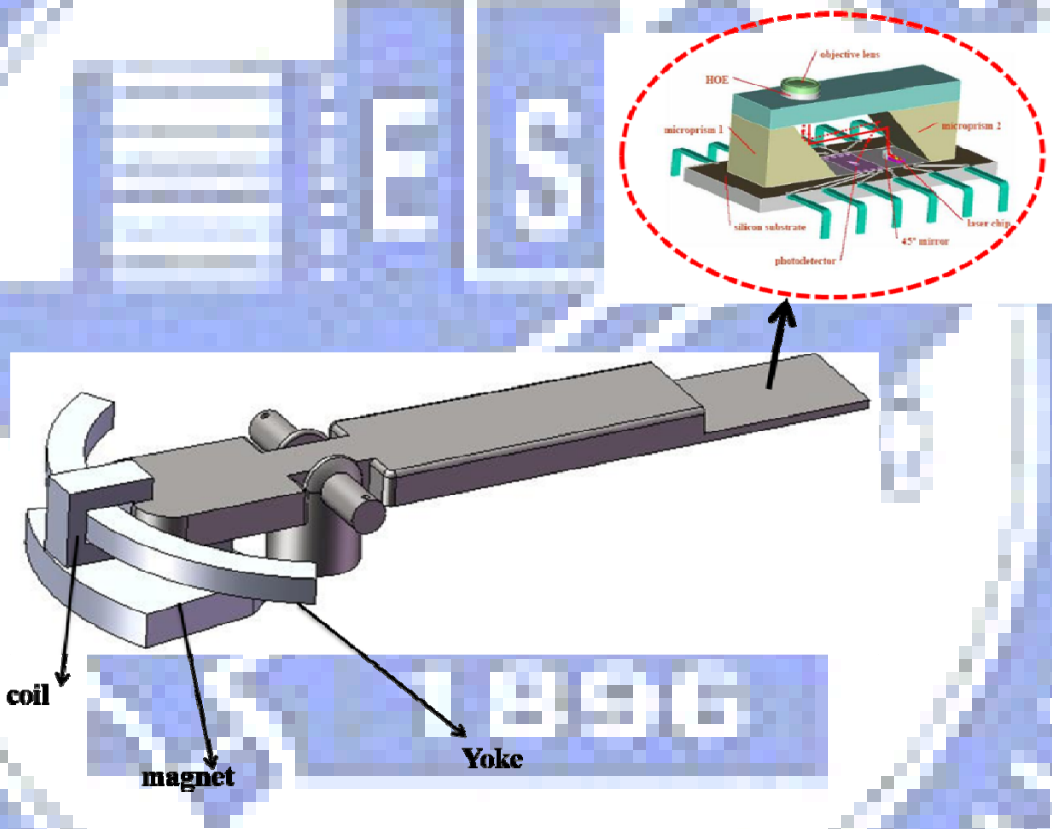

Fig. 1.1 dual-stage actuator

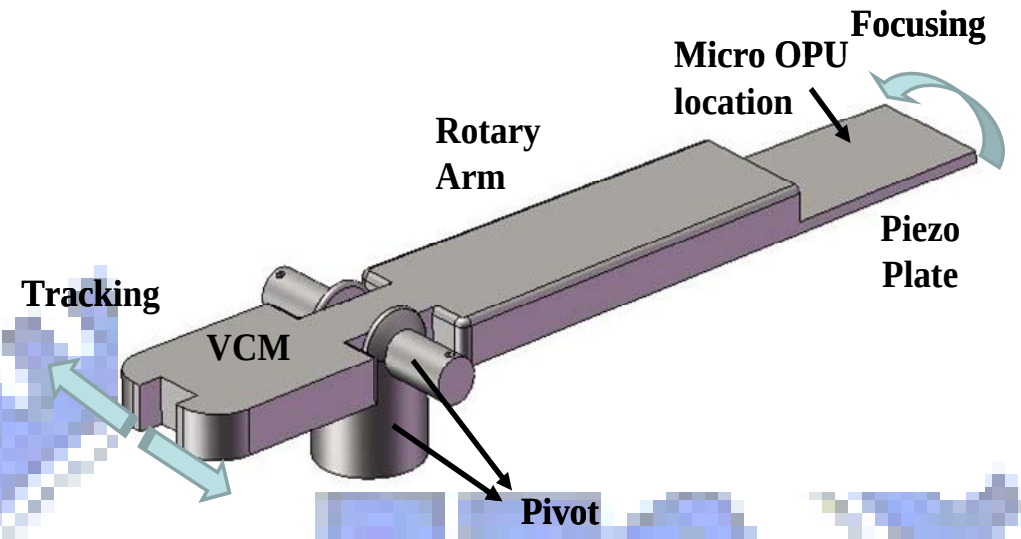

Fig. 1.2 dual-stage actuator action

1.2 Blue ray optical head

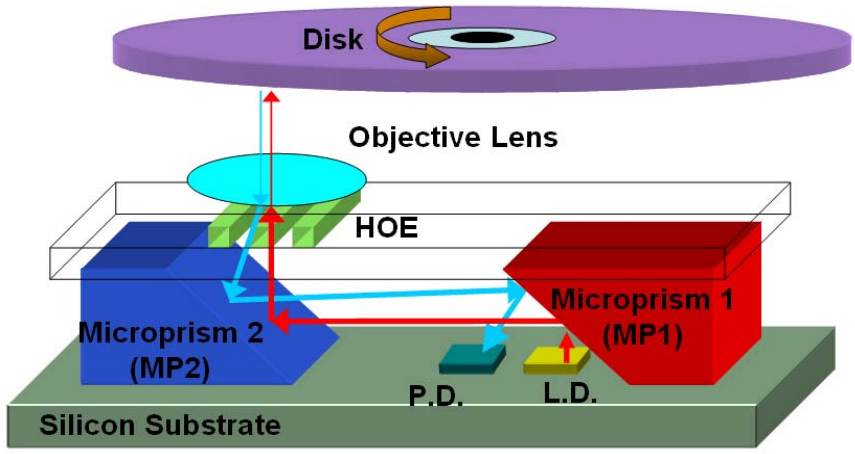

Fig. 1.3 Optical path of blue ray optical head

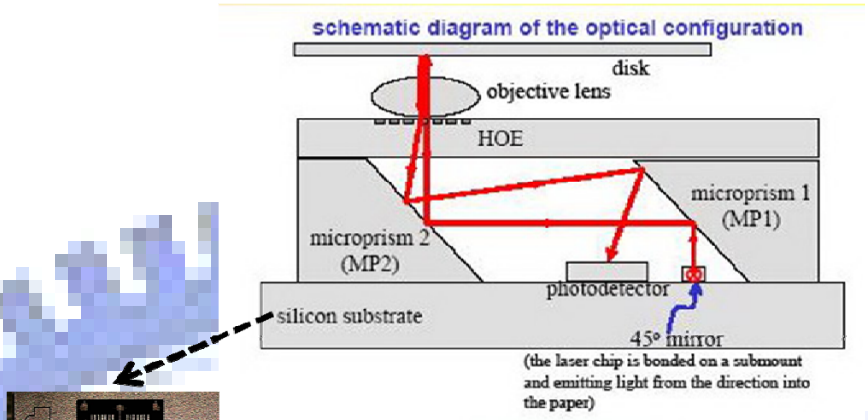

optical parameters

Item	Correspondence
image-object relation	finite-conjugate system
disc cover layer thickness	0 mm (surface recording)
laser wavelength	654nm
object NA (laser side)	0.1
image NA (disk side)	0.65
focal length	0.525μm
clear aperture diameter	1.0mm

Fig. 1.4 blue ray optical head 2

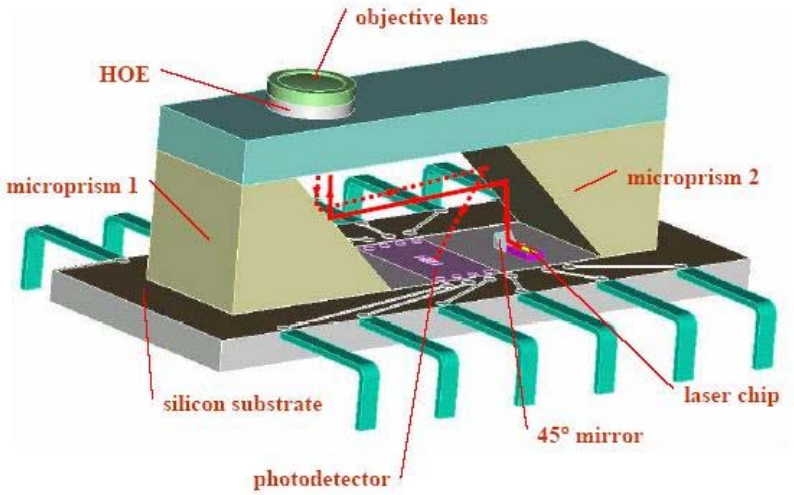

Fig. 1.5 blue ray optical head 3

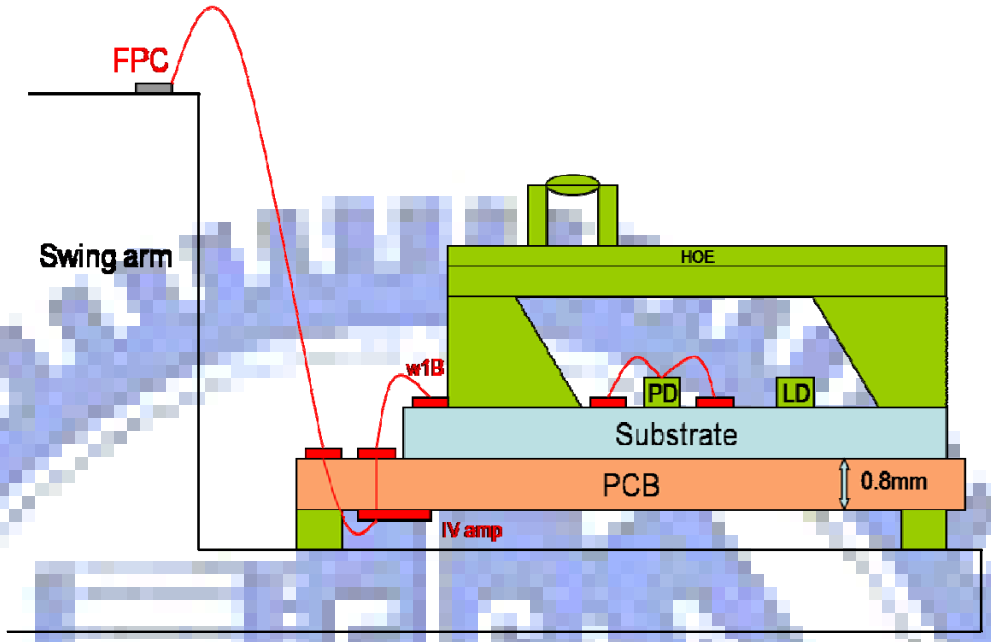

Fig. 1.6 optical head on seesaw actuator

There are two methods to improve the optical devices to exceed our hope. One method is improving the gain margin by analysis and redesign of VCM parameters [10]. It regulates the topology optimization and shape optimization of VCM. The VCM suspension design is to decrease the shock resistances and the equivalent mass with increasing first torsion frequency. The shape design is mass reduction for reducing power consumption [7] [9], and the position error signal (PES) would be maintained in minimum. Because of mini VCM structure and complex magnetic circuit, this mechanical design has some problems to decrease it thickness [10]. The complexity will not only impact the cost of the ODD but also degrade the servo performance owing to long delay time. A control problem is that the overshoot or oscillation may delay of the output signal and result in a long seeking time.

The other method is accomplished by control designed for robust performance [3]. The system must follow the track to keep the residual focusing error below its tolerance. Hence, the focusing servo system should keep the robust performance against sudden disturbance. Generally, the conventional tracking servo system is

accomplished by the feedback servo designed using PID control. It is difficult to compensate the sudden disturbance and periodic disturbance. The robust control and the adaptive control methods are used to eliminate the effects of uncertainty for systems with uncertainty. The adaptive control method has more applications in industrial and the robust control can effectively control systems with parameter uncertainty [7]. Recently, the several robust control has been realized by H∞ control theory, disturbance observer and so on. The robust control system based on H∞ control theory can keep a robust stable condition for parameter variation by its loop shaping [8] [9]. This paper focuses on a useful control loop, a two degree of freedom servo system is designed on the basis of doubly coprime factorization to consider the robust stability [8].

This paper is organized as follows. Section II used the robust tracking observer control system based on both two degree of freedom control system. Section III discusses the zero phase error tracking control (ZPETC) and a method of the system identification. Section IV gives a brief introduction on dual-stage servo system. Section V the new control method of ZPETC loop is in the dual stage robust control system. The performance of the proposed control scheme and experimental results are discussed in Section V. The conclusion is discussed in Section VI.

II. ROBUST DISTURBANCE OBSERVER ON 2DOF SERVO SYSTEM

2.1 Tracking control system

Significant progress in areal storage density of an ODD can be accomplished by using a dual-stage actuator system. In such a servo system a high-bandwidth and highly accurate micro actuator is used in combination with a traditional VCM to position the read/write head over the data track. The track following servo control system is required to perform robustly in the presence of uncertainties induced by disturbances and product variability. Because of the conventional is difficult to carry out the quick suppression of the sudden disturbance. The proposed two degree of freedom servo system considering the robust stability according to inertia variation is designed on the basis of Doubly Coprime Factorization and Disturbance Observer. For the design of a robust servo system, uncertainties are taken into account in the form of an uncertainty model. The uncertainty model consists of a nominal model together with an unknown but bounded description of the disturbances and uncertainty.

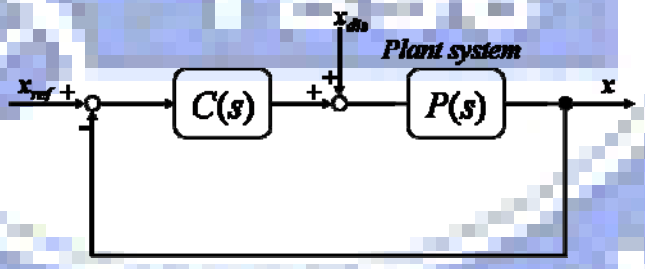

Fig. 2.1 tracking servo system for ODD

Generally, the block diagram of the tracking control system for an optical disk drive is shown in Fig2.1. Here, $P(s)$ is the tracking actuator for an optical disk drive, which is a moving-coil actuator. x_{ref} is the tracking position reference to be followed. x is the optical spot position. x_{dis} is a disturbance input.

2.2 Robust feedback controller based on disturbance observer

Based on coprime factorization, the transfer function $P(s)$ of the tracking actuator VCM and PZT are expressing by:

$$P(s) = \frac{N(s)}{D(s)} \tag{1}$$

$$\text{Bezout identity equation}: \; N(s) \cdot X(s) + D(s) \cdot Y(s) = 1 \tag{2}$$

The robust feedback controller $C(s)$ is determined by the coprime factorization $N(s)$, $D(s)$, $X(s)$, $Y(s)$.

$$C(s) = \frac{X(s) + Q(s)D(s)}{Y(s) - Q(s)N(s)} \tag{3}$$

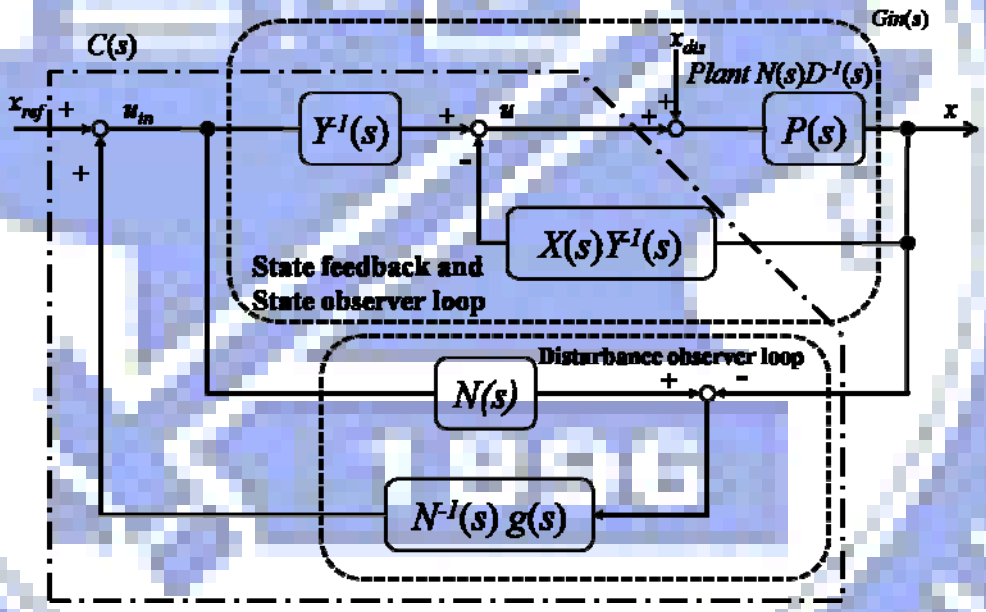

Fig. 2.2 Robust feedback controller based on disturbance observer

The free parameter $Q(s)$ in Eq.3 determines the disturbance rejection response $G_{dy}(s)$ of $g(s)$ and the robust stability condition. Generally, as the gains of $G_{dy}(s)$ and the sensitivity function $S(s)$ should become as small as possible in all frequency bandwidth and must be zero in steady state. This paper proposes that $Q(s)$ is determined by the stable and proper function $g(s)$. A gain of $g(s)$ is unity in steady state. The sensitivity function $S(s)$ and the disturbance rejection response $G_{dy}(s)$ are

represented as shown in (6) and (7). The block diagram of proposed robust control system is illustrated as shown in Fig. 2.2.

$$Q(s)=\frac{Y(s)}{N(s)}\cdot g(s),\ g(0)=1 \tag{4}$$

$$C(s)=\frac{X(s)+Q(s)\cdot D(s)}{Y(s)-Q(s)\cdot N(s)}=\frac{X(s)}{Y(s)}+\frac{g(s)}{N(s)\cdot Y(s)\cdot\left(1-g(s)\right)} \tag{5}$$

$$\text{Sesitivity function } S(s)=D(s)\cdot Y(s)\cdot\left[1-g(s)\right] \tag{6}$$

$$\text{Disturbance rejection response } G_{dy}(s)=N(s)\cdot Y(s)\cdot\left[1-g(s)\right] \tag{7}$$

Proof:

$$G_{in}(s):\ x=\frac{1}{Y(s)}\cdot\frac{P(s)}{1+\left(\frac{X(s)}{Y(s)}\cdot P(s)\right)}\cdot u_{in}+\frac{P(s)}{1+\left(\frac{X(s)}{Y(s)}\cdot P(s)\right)}x_{dis}$$

$$x=\left[\frac{P(s)}{Y(s)+X(s)\cdot P(s)}\right]\cdot u_{in}+\left[\frac{Y(s)\cdot P(s)}{Y(s)+X(s)\cdot P(s)}\right]\cdot x_{dis}$$

$$u_{in}=x_{ref}+\frac{g(s)}{N(s)}\cdot\left[N(s)\cdot u_{in}-x\right]\Rightarrow u_{in}=\frac{1}{1-g(s)}\cdot x_{ref}-\frac{1}{1-g(s)}\cdot\frac{g(s)}{N(s)}\cdot x$$

$$x=\left[\frac{P(s)}{Y(s)+X(s)\cdot P(s)}\right]\cdot\left[\frac{1}{1-g(s)}\cdot x_{ref}-\frac{1}{1-g(s)}\cdot\frac{g(s)}{N(s)}\cdot x\right]+\left[\frac{Y(s)\cdot P(s)}{Y(s)+X(s)\cdot P(s)}\right]\cdot x_{dis}$$

$$x=\frac{N(s)\cdot P(s)\cdot x_{ref}+N(s)\cdot Y(s)\cdot\left(1-g(s)\right)\cdot P(s)\cdot x_{dis}}{N(s)\cdot Y(s)\cdot\left(1-g(s)\right)+\left[N(s)\cdot X(s)\cdot\left(1-g(s)\right)+g(s)\right]\cdot P(s)}$$

$$x=\frac{\frac{N(s)\cdot P(s)\cdot x_{ref}}{N(s)\cdot Y(s)\cdot\left[1-g(s)\right]}+P(s)\cdot x_{dis}}{1+\frac{\left[N(s)\cdot X(s)\cdot\left[1-g(s)\right]+g(s)\right]\cdot P(s)}{N(s)\cdot Y(s)\cdot\left[1-g(s)\right]}}=\frac{\frac{N(s)\cdot P(s)\cdot x_{ref}}{N(s)\cdot Y(s)\cdot\left[1-g(s)\right]}+P(s)\cdot x_{dis}}{1+\left[\frac{X(s)}{Y(s)}+\frac{g(s)}{N(s)\cdot Y(s)\cdot\left[1-g(s)\right]}\right]\cdot P(s)}$$

$$x=\frac{N(s)\cdot\frac{N(s)}{D(s)}\cdot x_{ref}}{1+\left[\frac{X(s)}{Y(s)}+\frac{g(s)}{N(s)\cdot Y(s)\cdot\left[1-g(s)\right]}\right]\cdot\frac{N(s)}{D(s)}}+\frac{\frac{N(s)}{D(s)}\cdot x_{dis}}{1+\left[\frac{X(s)}{Y(s)}+\frac{g(s)}{N(s)\cdot Y(s)\cdot\left[1-g(s)\right]}\right]\cdot\frac{N(s)}{D(s)}}=\frac{\frac{N(s)\cdot x_{ref}+N(s)\cdot Y(s)\cdot\left[1-g(s)\right]\cdot x_{dis}}{D(s)\cdot Y(s)\cdot\left[1-g(s)\right]}}{1+\left[\frac{N(s)\cdot X(s)}{D(s)\cdot Y(s)}+\frac{g(s)}{D(s)\cdot Y(s)\cdot\left[1-g(s)\right]}\right]}$$

$$x=\frac{\frac{N(s)\cdot x_{ref}+N(s)\cdot Y(s)\cdot\left[1-g(s)\right]\cdot x_{dis}}{D(s)\cdot Y(s)\cdot\left[1-g(s)\right]}}{\frac{1}{D(s)\cdot Y(s)\cdot\left[1-g(s)\right]}\cdot\left[D(s)\cdot Y(s)\cdot\left[1-g(s)\right]+N(s)\cdot X(s)\cdot\left[1-g(s)\right]+g(s)\right]}$$

$$x = \left[D(s) \cdot Y(s) \cdot \left[1 - g(s)\right] \right] \cdot \frac{N(s) \cdot x_{ref} + N(s) \cdot Y(s) \cdot \left[1 - g(s)\right] \cdot x_{dis}}{D(s) \cdot Y(s) \cdot \left[1 - g(s)\right]}$$

2.3 Robust stability condition

The inner loop is the closed loop system based on the state feedback and the state observer. The outer loop system is equivalent to the closed loop system based on disturbance observer. Fig. 2.2 points out that $g(s)$ is equivalent to the low pass filter of the conventional disturbance observer and defines the complementary sensitivity function $T(s)$ of the outer loop system. $[1-g(s)]$ is the sensitivity function of the outer loop system, and $[N(s) \cdot Y(s)]$ is the sensitivity function of the inner loop.

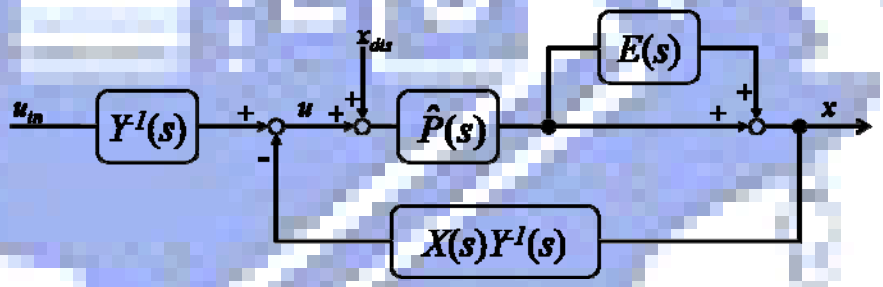

Fig. 2.3 multiple perturbation of inner loop

Since the lower resonant frequency is dominant for the frequency characteristics of the tracking actuator, we use the following approximation:

$$\hat{P}(s) = \frac{K_a}{M \cdot s^2 + D \cdot s + K_s}$$

K_a, M, D and K_s are the force constant, the mass of the moving parts of the actuator, and the viscosity coefficient and the spring modulus. We denote $P(s)$ as $\hat{P}(s)$ when these parameters are nominal. Taking multiplicative perturbation $E(s)$ into account, the model is given by:

$$P(s) = \hat{P}(s) \cdot \left[1 + E(s)\right] \tag{8}$$

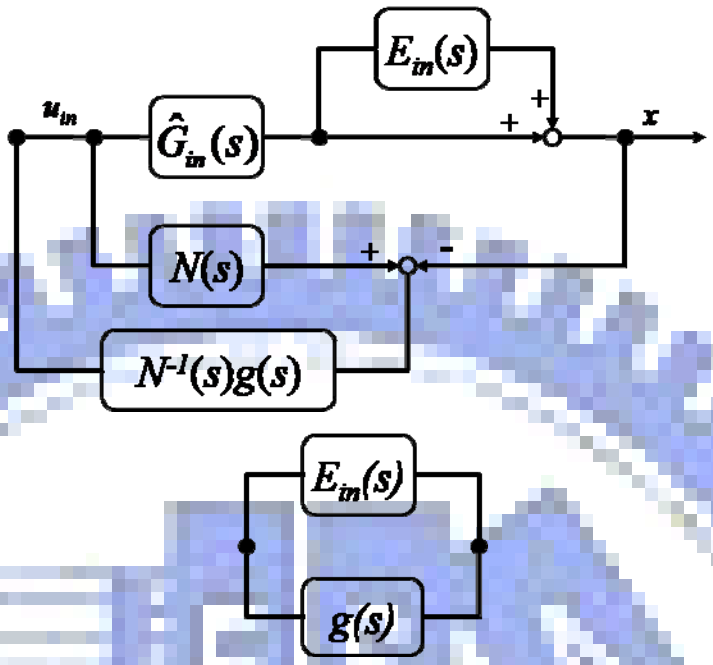

Fig. 2.4 robust stability condition

The dynamics fluctuation $E_{in}(s)$ of the inner loop system is represented as shown in (9) and Fig. 2.4 $\hat{G}_{in}(s)$ is the nominal dynamics of $G_{in}(s)$, and it becomes $N(s)$. In order to keep the robust stable condition, the multipliable perturbation $E_{in}(s)$ needs to be a stable function. When the gain of $g(s)$ is smaller than that of the multipliable perturbation $E_{in}^{-1}(s)$ in all frequency, the proposed system keeps the robust stability.

$$G_{in}(s) = \hat{G}_{in}(s)\cdot\left[1+E_{in}(s)\right] = \hat{G}_{in}(s)\cdot\left[1+\frac{Y(s)\cdot D(s)\cdot E(s)}{1+N(s)\cdot X(s)\cdot E(s)}\right] \tag{9}$$

Proof:

$$x = \frac{1}{Y(s)}\cdot\frac{P(s)\cdot\left[1+E(s)\right]}{1+\frac{X(s)}{Y(s)}\cdot P(s)\cdot\left[1+E(s)\right]}\cdot u_{in} + \frac{P(s)\cdot\left[1+E(s)\right]}{1+\frac{X(s)}{Y(s)}\cdot P(s)\cdot\left[1+E(s)\right]}\cdot x_{dis}$$

$$x = \frac{1}{Y(s)}\cdot\frac{\frac{N(s)}{D(s)}\left[1+E(s)\right]}{1+\frac{X(s)}{Y(s)}\cdot\frac{N(s)}{D(s)}\cdot\left[1+E(s)\right]}\cdot u_{in} + \frac{\frac{N(s)}{D(s)}\cdot\left[1+E(s)\right]}{1+\frac{X(s)}{Y(s)}\cdot\frac{N(s)}{D(s)}\cdot\left[1+E(s)\right]}\cdot x_{dis}$$

$$x = \frac{N(s)\cdot[1+E(s)]\cdot u_{in} + N(s)\cdot Y(s)\cdot[1+E(s)]\cdot x_{dis}}{D(s)\cdot Y(s) + N(s)\cdot X(s)\cdot[1+E(s)]}$$

$$x = \frac{N(s)\cdot[1+E(s)]\cdot u_{in} + N(s)\cdot Y(s)\cdot[1+E(s)]\cdot x_{dis}}{1+N(s)\cdot X(s)\cdot E(s)}$$

$$x = \hat{G}_{in}(s)\cdot\frac{1+E(s)}{1+N(s)\cdot X(s)\cdot E(s)}\cdot[u_{in} + Y(s)\cdot x_{dis}]$$

$$x = \hat{G}_{in}(s)\cdot\left\{\frac{1+[N(s)\cdot X(s)+Y(s)\cdot D(s)]\cdot E(s)}{1+N(s)\cdot X(s)\cdot E(s)}\right\}\cdot[u_{in} + Y(s)\cdot x_{dis}]$$

$$x = \hat{G}_{in}(s)\cdot\left\{1+\frac{Y(s)\cdot D(s)\cdot E(s)}{1+N(s)\cdot X(s)\cdot E(s)}\right\}\cdot[u_{in} + Y(s)\cdot x_{dis}]$$

For the purpose of satisfying the robust stability condition (9) and stabilizing the $E_{in}(s)$, this paper suitably designs $g(s)$, the gains of state feedback and state observer.

$$\|E_{in}(s)\cdot g(s)\|_{\infty} < 1 \tag{10}$$

Proof:

$$\left\{N(s)\cdot u_{in} - \left[\hat{G}_{in}(s)\cdot(1+E_{in}(s))\right]\cdot u_{in}\right\}\cdot\frac{g(s)}{N(s)}$$

$$\left\{N(s)\cdot u_{in} - \left[N(s)\cdot(1+E_{in}(s))\right]\cdot u_{in}\right\}\cdot\frac{g(s)}{N(s)} = -E_{in}(s)\cdot g(s)$$

Moreover, as the robust control system is requested to keep the desired disturbance rejection response $G_{dy}(s)$, the proposed system should consider the perturbation of $G_{dy}(s)$ caused by the parameter variation. The dynamical model of disturbance input signal is $x_{dis}(s)$. Moreover, the position disturbance $x_{pd}(s)$ caused by $x_{dis}(s)$ can he defined as shown in Eq11. Hence, the disturbance suppression response $G_{dy}(s)$ of tested servo system is determined by Eq.12.

$$x_{pd}(s) = \frac{K_a}{M\cdot s^2 + D\cdot s + K_s}\cdot x_{dis}(s) \tag{11}$$

$$G_{dy}(s) = \frac{x(s)}{x_{pd}(s)} = D(s)\cdot Y(s)\cdot[1-g(s)] \tag{12}$$

Proof:

$$x_{pd}(s) = P(s) \cdot x_{dis}(s) = \frac{N(s)}{D(s)} \cdot x_{dis}(s)$$

$$x(s) = D(s) \cdot Y(s) \cdot [1 - g(s)] \cdot x_{pd}(s) = D(s) \cdot Y(s) \cdot [1 - g(s)] \cdot \frac{N(s)}{D(s)} \cdot x_{dis}(s)$$

$x(s) = \underbrace{N(s) \cdot Y(s) \cdot [1 - g(s)]}_{G_{dy}(s)} \cdot x_{dis}(s)$ is equal to Eq.7

The tested robust feedback controller $C(s)$ keeps both the desired robust stable condition for parameter variations and the desired disturbance suppression response. In order to realize these robust control performances of $C(s)$, this paper satisfies the both equations Eq.13. ε is the gain margin of the disturbance suppression response. When ε is small, the tested robust feedback controller $C(s)$ has a disturbance suppression response. In this paper, the feedback controller $C(s)$ satisfies both the robust stability condition on $\pm 20\%$ multiplicative perturbation of spring constant K_s, and the sensitivity function $S(s)$ becomes -60dB around 100[rad/sec]. Therefore, the gain margin ε is 0.01, and the poles of tested robust feedback controller $C(s)$ are determined as shown in system ID.

$$\left\| x_{pd}(s) \cdot S(s) \right\|_{\infty} < \varepsilon \tag{13}$$

$$\left\| x_{pd}(s) \cdot \{ D(s) \cdot Y(s) \cdot [1 - g(s)] \} \right\|_{\infty} < \varepsilon$$

$$|1 - g(s)| < \left| \varepsilon \cdot \left[D(s) \cdot Y(s) \cdot x_{pd}(s) \right]^{-1} \right|$$

2.4 2DOF control System

The robust control system based on disturbance observer has sometimes a high overshoot and an oscillated response. In order to overcome these problems, this paper proposes a new two-degrees-of-freedom control system based on doubly coprime factorization.

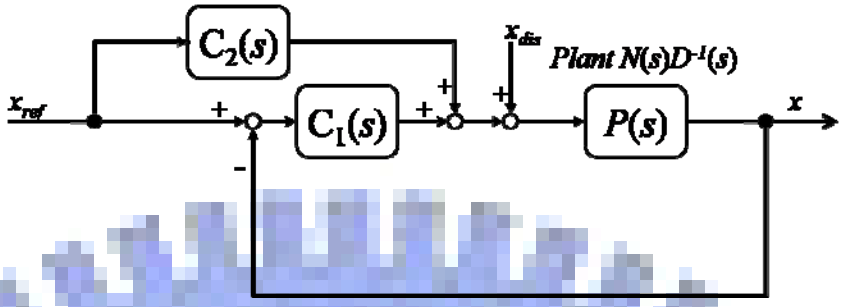

Fig. 2.5 General model of 2DOF control System

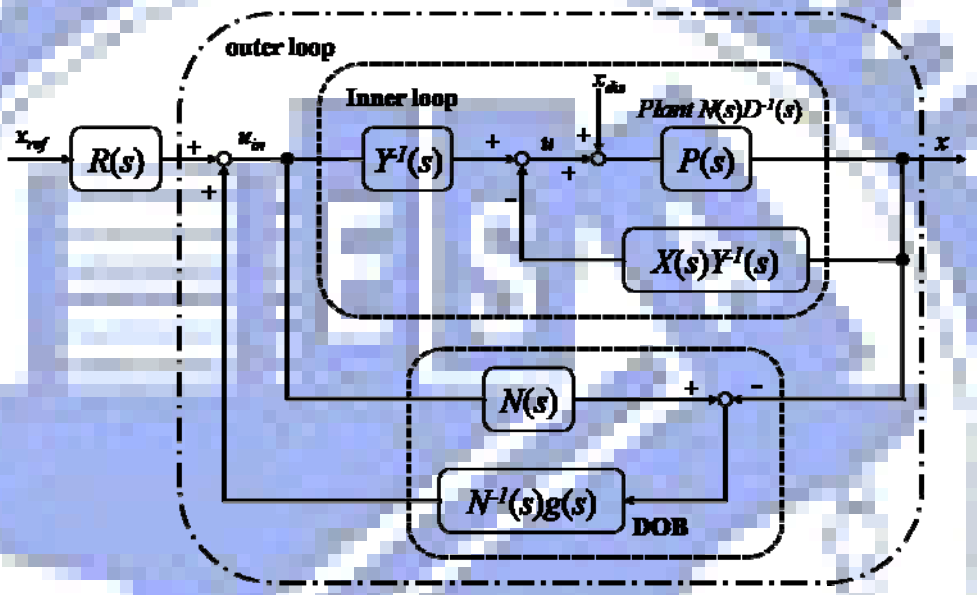

Fig. 2.6 2DOF Control System

Where, $P(s)$ denotes the plant to be controlled. The feedback compensator $C_1(s)$ defines both the disturbance rejection response $G_{dy}(s)$ and a robust stability. The feed-forward compensator $C_2(s)$ defines a reference input response $G_{ry}(s)$. It is obvious that the feed-forward compensator $C_2(s)$ is not able to improve the stability of the closed-loop system. Therefore, the feedback controller $C_1(s)$ must be designed to stabilize the feedback system composed of $P(s)$ and $C_1(s)$.

$$G_{dy}(s) = N(s) \cdot Y(s) \cdot [1 - g(s)]$$

$$G_{ry}(s) = N(s) \cdot R(s)$$

$$S(s) = D(s) \cdot Y(s) \cdot [1 - g(s)]$$

Proof:

$$G_{in}(s):\ x=\frac{1}{Y(s)}\cdot\frac{\frac{N(s)}{D(s)}}{1+\left(\frac{X(s)}{Y(s)}\cdot\frac{N(s)}{D(s)}\right)}\cdot u_{in}+\frac{\frac{N(s)}{D(s)}}{1+\left(\frac{X(s)}{Y(s)}\cdot\frac{N(s)}{D(s)}\right)}x_{dis}$$

$$x=N(s)\cdot u_{in}+N(s)\cdot Y(s)\cdot x_{dis}$$

$$u_{in}=R(s)\cdot x_{ref}+\frac{g(s)}{N(s)}\cdot\left[N(s)\cdot u_{in}-x\right]\Rightarrow u_{in}=\frac{R(s)}{1-g(s)}\cdot x_{ref}-\frac{1}{1-g(s)}\cdot\frac{g(s)}{N(s)}\cdot x$$

$$x=N(s)\cdot\left[\frac{R(s)}{1-g(s)}\cdot x_{ref}-\frac{1}{1-g(s)}\cdot\frac{g(s)}{N(s)}\cdot x\right]+N(s)\cdot Y(s)\cdot x_{dis}$$

$$x=N(s)\cdot R(s)\cdot x_{ref}+N(s)\cdot Y(s)\cdot\left[1-g(s)\right]\cdot x_{dis}$$

$$C_2(s)=D(s)\cdot R(s)+C_1(s)\cdot\left[N(s)\cdot R(s)-1\right]$$

Proof:

$$N(s)\cdot R(s)\cdot x_{ref}=\frac{\left[C_1(s)+C_2(s)\right]\cdot P(s)}{1+C_1(s)\cdot P(s)}\cdot x_{ref}=\frac{\left[C_1(s)+C_2(s)\right]\cdot N(s)}{D(s)+C_1(s)\cdot N(s)}\cdot x_{ref}$$

$$R(s)\cdot x_{ref}=\frac{\left[C_1(s)+C_2(s)\right]}{D(s)+C_1(s)\cdot N(s)}x_{ref}$$

$$\left[D(s)\cdot R(s)+C_1(s)\cdot N(s)\cdot R(s)\right]\cdot x_{ref}=\left[C_1(s)+C_2(s)\right]\cdot x_{ref}$$

$$C_2(s)=D(s)\cdot R(s)+C_1(s)\cdot\left[N(s)\cdot R(s)-1\right]$$

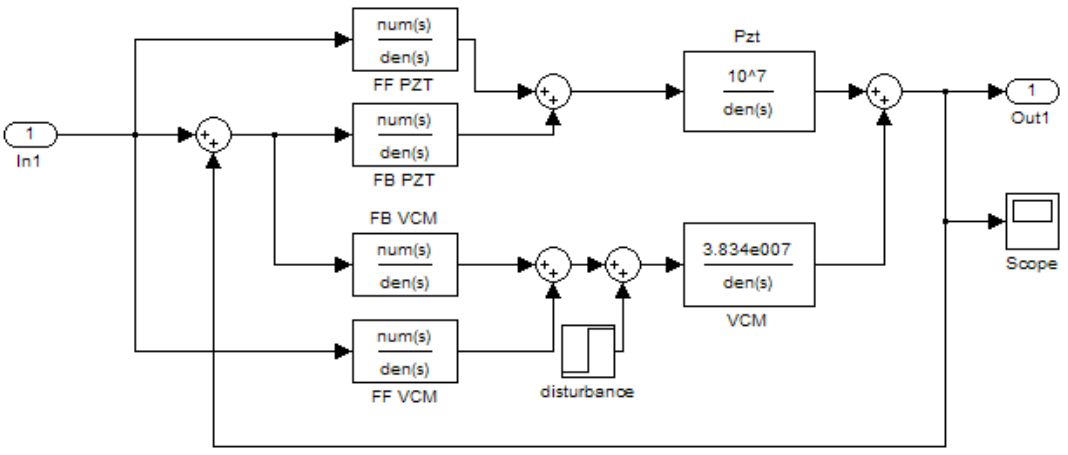

Fig. 2.7.sudden disturbance model

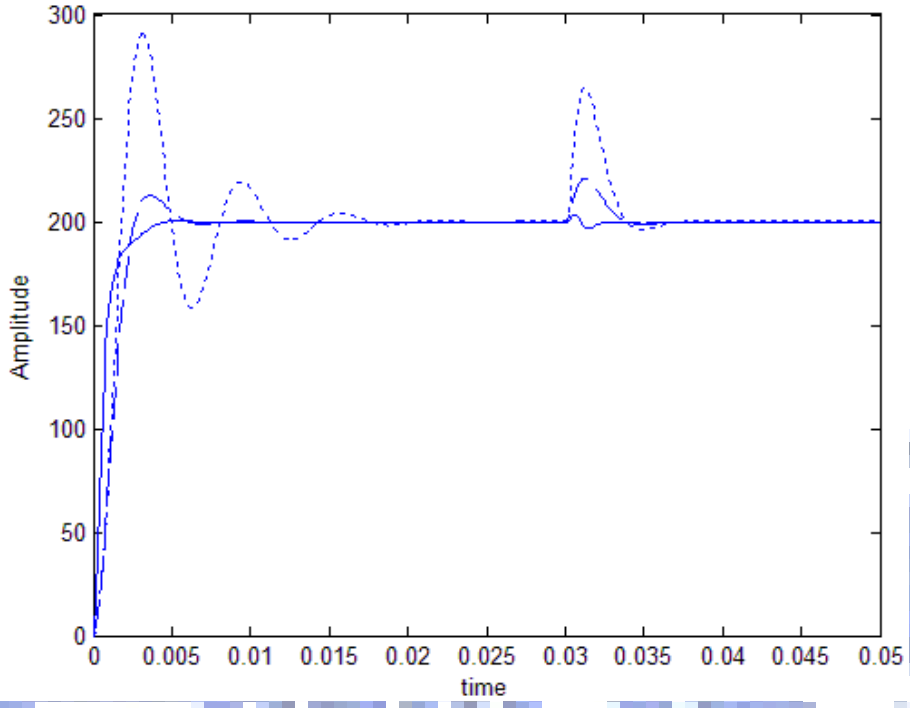

Fig. 2.8.step response

For the purpose of satisfying the robust stability Eq.12 and stabilizing the $E_{in}(s)$, this paper suitably designs the LPF $g(s)$. In order to identify the disturbance rejection, we add the sudden disturbance (100amplitude at 0.03 second) to VCM. In Fig. 2.5, we compare the PID control (dotted line), the simple robust control (dashed line), and the 2DOF of the robust control (Solid line). The 2DOF servo system can usefully reject the sudden disturbance.

III ZERO PHASE ERROR TRACKING CONTROL AND SYSTEM IDENTIFICATION

3.1 feed-forward control system

A control problem is that the overshoot or oscillation may delay of the output signal and result in a long seeking time. Solving this problem can use the ZPET Controller to repair the phase error and delay. The ZPETC design method was proposed by Tomizuka [10] to improve tracking accuracy in feedback control loop. The design of the ZPETC controller directly cancels the stable (well – damped) poles and zeros in the position feedback loop and compensates for the unstable zeros to achieve the zero phase error in the servo system [4]. Recently, the Miniaturized Optical Disc Drive has been realized by ZPET control system. This is a new developed methods involve compensation for all undesired zeros or heavy computations [2] [3]. This system has been shown to reduce residual focusing error far better than conventional feedback control, and has demonstrated the capability to reduce the residual focusing error [5]. The feed-forward controller desires to track any time varying output signal without the phase error. Those uncertain item and delay time produce the phase error. Although it is further assumed that a feedback controller remains system stable, the feed-forward controller is useful to achieve a good tracking performance fast.

In the past, this pole-zero cancellation method was not approach to stable to any condition. If there exist non-minimum phase zeros in the transfer function to be controlled, this method is no doubt make the actuator unstable. The pole-zero cancellation method only cancels those stable zeros and poles, but the system still have phase lag between the actual output signal and the desired tracking signal.

Tomizuka (1987) solved this control problem from the frequency response and designed a new type of feed-forward controller. The proposed feed-forward control system can reduce the tracking error caused by time delay.

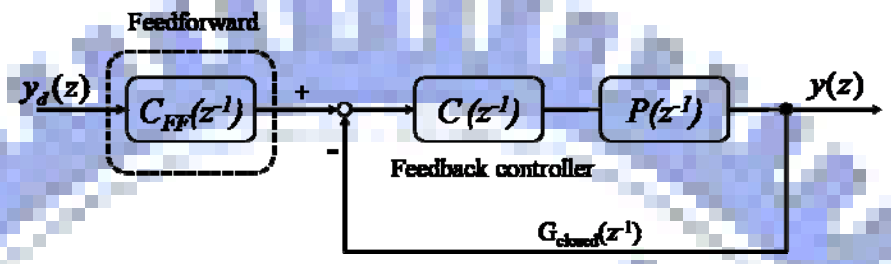

Fig. 3.1 feed-forward control system

It supposes the feedback closed loop transfer function in the discrete time. The transfer function includes the stable plant (actuator) and feedback controller. Referring Fig.3.1 the transfer function write down as:

$$G_{closed}(z^{-1}) = \frac{C(z^{-1}) \cdot P(z^{-1})}{1 + C(z^{-1}) \cdot P(z^{-1})} = \frac{z^{-d} \cdot \overbrace{B_c(z^{-1})}^{\text{function numerator}}}{\underbrace{A_c(z^{-1})}_{\text{function denominator}}} \tag{14}$$

Where

$$A_c(z^{-1}) = 1 + a_{c1}z^{-1} + a_{c2}z^{-2} + a_{c3}z^{-3} + \ldots + a_{cn}z^{-n}$$

$$B_c(z^{-1}) = b_{c0} + b_{c1}z^{-1} + b_{c2}z^{-2} + b_{c3}z^{-3} + \ldots + b_{cm}z^{-m}, \; b_{c0} \neq 0$$

$A_c(z^{-1})$ and $B_c(z^{-1})$ are the stable polynomials of the Z-transform.

z^{-d} is the time delay of that uncertain disturbance which makes the unnecessary delay of machine.

3.2 phase pre-compensator design

Fig. 3.2 describes the phase pre-compensator design of the dynamic system. It uses the poles-zeros cancellation method which the closed loop have the stable zeros.

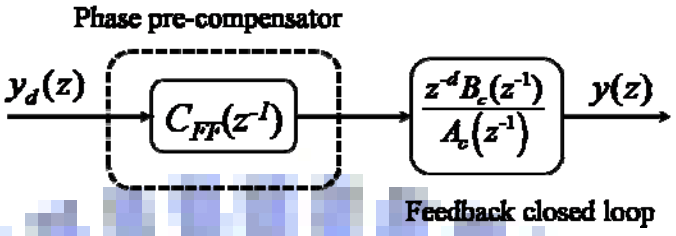

Fig. 3.2 Feed-Forward (FF) controller

$$C_{FF}(z^{-1}) = \frac{1}{G_{closed}(z^{-1})} = \frac{z^d \cdot A_c(z^{-1})}{B_c(z^{-1})} \tag{15}$$

The term z^d represent to a d-step lead of the transfer function. The step lead z^d used to compensate the system delay. z^d made the input signal $y_d(z)$ to the d step lead signal $z^d \cdot y_d(z)$.

$$y(z) = C_{FF}(z^{-1}) \cdot G_{closed}(z^{-1}) = \left[\frac{z^d \cdot A_c(z^{-1})}{B_c(z^{-1})}\right] \cdot \left[\frac{z^{-d} \cdot B_c(z^{-1})}{A_c(z^{-1})}\right] \cdot y_d(z) = y_d(z) \tag{16}$$

When the output signal $y(z)$ equal to the input signal $y_d(z)$, the system with feed-forward controller can track any time varying signal without have the phase shifted.

3.3 ZPETC controller

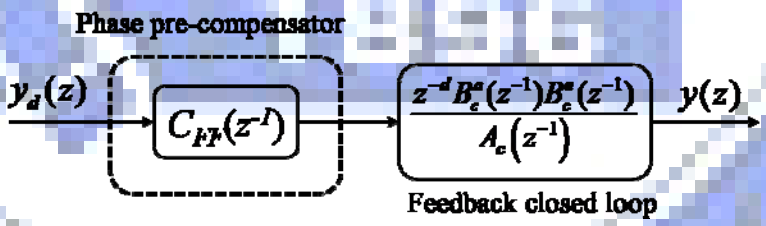

Fig. 3.3 Feed-forward controller design

The closed loop transfer function divides into two terms, the controllable item and the non-controllable item. The linear transfer function consists of the controllable poles and zeros. The stable poles and zeros take the error signal approximate to zero in infinite. And the non-controllable transfer function consists of all unstable zeros. The unstable zeros include both non-minimum phase zeros and overly oscillatory

zeros. Those unstable zeros cause the errors signals which passing the feed-forward controller explode or exceeding the oscillation of the plant. It takes the new function numerator $\left[B_c^a(z^{-1})\cdot B_c^u(z^{-1})\right]$ to replace the old numerator $B_c(z^{-1})$.

When the transfer function of the closed-loop system of the feedback control system is $G_{closed}(z^{-1})$, and we divided the zeros of the $G_{closed}(z^{-1})$ into two parts:

$$G_{closed}\left(z^{-1}\right)=\frac{z^{-d}\cdot B_c\left(z^{-1}\right)}{A_c\left(z^{-1}\right)}=\frac{z^{-d}B_c^a(z^{-1})B_c^u(z^{-1})}{A_c\left(z^{-1}\right)} \tag{17}$$

$$B_c^a(z^{-1})=b_{c0}^a+b_{c1}^a z^{-1}+b_{c2}^a z^{-2}+b_{c3}^a z^{-3}+\ldots+b_{cq}^a z^{-q}\ ,\ b_{c0}^a\neq 0$$

$$B_c^u(z^{-1})=b_{c0}^u+b_{c1}^u z^{-1}+b_{c2}^u z^{-2}+b_{c3}^u z^{-3}+\ldots+b_{cp}^u z^{-p},\ b_{c0}^u\neq 0$$

$$q+p=m,\ \text{and}\ \ B_c(z^{-1})=B_c^a(z^{-1})\cdot B_c^u(z^{-1})$$

$B_c^a(z^{-1})$ has all accepted zeros.

$B_c^u(z^{-1})$ include the plant zeros outside and on the unit circle of the complex plane.

Referring Eq.17, the ZPET feed-forward controller is expressed as:

$$C_{FF}\left(z^{-1}\right)=\frac{z^d A_c\left(z^{-1}\right)}{B_c\left(z^{-1}\right)}=\frac{z^d A_c(z^{-1})}{B_c^a(z^{-1})\cdot B_c^u(z^{-1})} \tag{18}$$

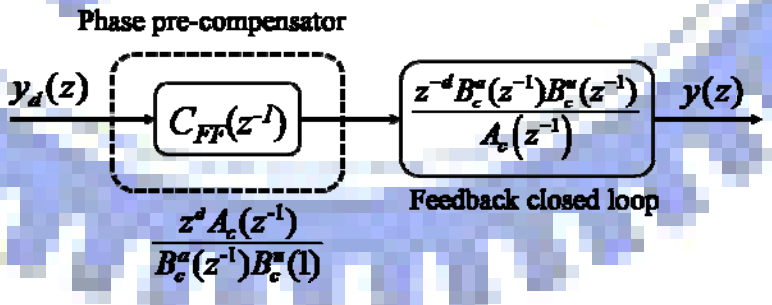

Fig. 3.4 Feed-forward controller

Although the closed loop has the unstable zeros, the frequency response remains approach to stable without explode and unstable.

$$C_{FF}\left(z^{-1}\right)=\frac{z^{d}A_c(z^{-1})}{B_c^{a}(z^{-1})B_c^{u}(z^{-1})}=\frac{z^{d}A_c(z^{-1})}{B_c^{a}(z^{-1})B_c^{u}(1)} \tag{19}$$

$$y(z)=\left[\frac{z^{d}A_c(z^{-1})}{B_c^{a}(z^{-1})\cdot B_c^{u}(1)}\cdot y_d(z)\right]\cdot\frac{z^{-d}\cdot B_c^{a}(z^{-1})\cdot B_c^{u}(z^{-1})}{A_c(z^{-1})}=\frac{B_c^{u}(z^{-1})}{B_c^{u}(1)}\cdot y_d(z) \tag{20}$$

The prefect control makes $\frac{B_c^{u}(z^{-1})}{B_c^{u}(1)}\cdot y_d(z)$ equal to $y(z)$. In this desired situation, the phase shifted will disappear and approach to neglect. But the polynomial of the unstable zeros $B_c^{u}(z^{-1})$ is not easy to handle. It takes $y_d'(z)=\frac{B_c^{u}(z)}{B_c^{u}(1)}\cdot y_d(z)$ to the substitution for $y(z)=\frac{B_c^{u}(z^{-1})}{B_c^{u}(1)}\cdot y_d(z)$.

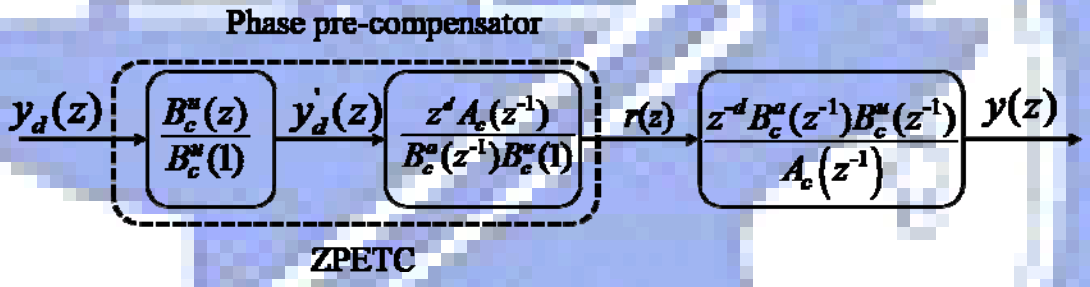

Fig. 3.5 ZPETC controller

$$y(z)=\frac{B_c^{u}(z)}{B_c^{u}(1)}\cdot\left[\frac{z^{d}A_c(z^{-1})}{B_c^{a}(z^{-1})\cdot B_c^{u}(1)}\right]\cdot\frac{z^{-d}\cdot B_c^{a}(z^{-1})\cdot B_c^{u}(z^{-1})}{A_c(z^{-1})}\cdot y_d(z)$$

$$y(z)=\frac{B_c^{u}(z)B_c^{u}(z^{-1})}{B_c^{u}(1)^{2}}\cdot y_d(z) \tag{21}$$

$$\left|\frac{B_c^{u}(z^{-1})\cdot B_c^{u}(z)}{B_c^{u}(1)^{2}}\cdot y_d(z)\right|=R_e(\omega)^2+I_m(\omega)^2\neq 0 \tag{22}$$

Eq.22 shows the degree of the transfer function in the complex plane:

$$\left.\frac{B_c^{u}(z)}{B_c^{u}(1)}\right|_{z=e^{jwT}}=R_e(w)+jI_m(w) \tag{23}$$

$$\left.\frac{B_c^u(z^{-1})}{B_c^u(1)}\right|_{z=e^{j\omega T}} = R_e(\omega) - jI_m(\omega) \tag{24}$$

$$\angle\frac{B_c^u(z)}{B_c^u(1)} + \angle\frac{B_c^u(z^{-1})}{B_c^u(1)} = \tan^{-1}\left[\frac{I_m(\omega)}{R_e(\omega)}\right] - \tan^{-1}\left[\frac{I_m(\omega)}{R_e(\omega)}\right] = 0 \tag{25}$$

Eq.24 and Eq.25 make the phase error approach to the minimum. The actual output signals will track to the time varying signals. Even if the control method is effective to handle the unstable zeros in the feed-forward controller, but also it still has an inevitable magnitude $R_e(\omega)^2 + I_m(\omega)^2$ in the ZPETC controller.

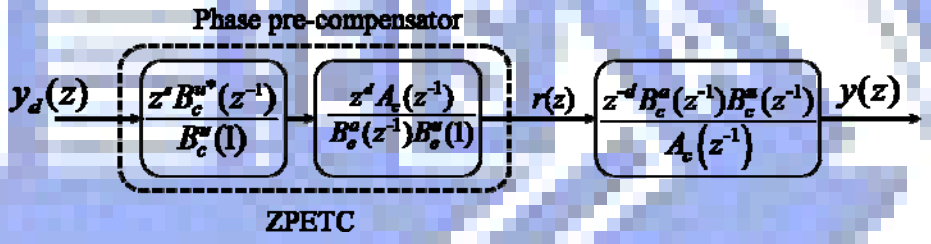

Fig. 3.6 ZPECT controller

From Fig.3.5 the ZEPTC is express as:

$$r(z) = \left[\frac{B_c^u(z)}{B_c^u(1)}\right]\cdot\left[\frac{z^d A_c(z^{-1})}{B_c^a(z^{-1})B_c^u(1)}\right]\cdot y_d(z) = \frac{z^d A_c(z^{-1})\cdot B_c^u(z)}{B_c^a(z^{-1})\cdot B_c^u(1)^2}\cdot y_d(z) \tag{26}$$

Eq.26 will replace the polynomial $B_c^u(z)$ to the polynomial $B_c^{u*}(z^{-1})$:

$$B_c^u(z) = b_{c0}^u + b_{c1}^u\cdot z + b_{c2}^u\cdot z^2 + b_{c3}^u\cdot z^3 + b_{c4}^u\cdot z^4 + b_{c5}^u\cdot z^5 + b_{c6}^u\cdot z^6 + \ldots$$

$$B_c^{u*}(z^{-1}) = b_{c0}^{u*} + b_{c1}^{u*}\cdot z^{-1} + b_{c2}^{u*}\cdot z^{-2} + b_{c3}^{u*}\cdot z^{-3} + b_{c4}^{u*}\cdot z^{-4} + b_{c5}^{u*}\cdot z^{-5} + b_{c6}^{u*}\cdot z^{-6} + \ldots$$

$$B_c^u(z) = B_c^{u*}(z^{-1})\cdot z^s$$

where s is the maximum order of z polynomial (27)

$$r(k) = \frac{z^d A_c(z^{-1})\cdot B_c^u(z)}{B_c^a(z^{-1})\cdot B_c^u(1)^2}\cdot y_d(z) = \frac{z^{d+s} A_c(z^{-1})\cdot B_c^{u*}(z^{-1})}{B_c^a(z^{-1})\cdot B_c^u(1)^2}\cdot y_d(z) \tag{28}$$

z^{d+s} can estimate $d+s$ step to compensate the closed loop delay time in advance.

3.4 System Identification

Designed ZPETC need the useful inverse model, so we investigated a more accurate control model by comparing the tracking characteristics of VCM and PZT in the ZPETC loop. A model is the knowledge of the properties of a system, and it is necessary to solve problems of control, signal processing, system design. Sometimes a simple model is useful for explaining certain phenomena.

A model may be given in three following forms:

- Knowledge of the system's behavior is summarized in a person's mind.
- Graphs and tables: e.g. the step response, Bode plot, closed-loop block diagram.
- Mathematical models: Here it confines this class of model to differential and difference equations, or it can used state equation to solve the dynamically system.

There are two ways constructing mathematical models.

A. Physical modeling:

   Newton's laws from physics such as balance equations are used to describe the dynamical behavior of a process. In many cases the processes are so complex that it is not possible to obtain reasonable models using only physical analyze.

B. System identification:

   Some experiments are performed on the system. A model is fitted to the output data by assigning accepted values to model parameters. System identification is the field of modeling dynamic systems from experimental data.

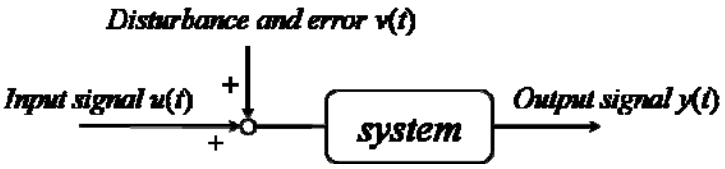

Fig. 3.7 dynamical model

The system is controlled by input signal $u(t)$. But the nonlinear disturbance $v(t)$ exists in the dynamical system, and it is hard to reduce the outside disturbance. A useful model should encompass essential characteristic without becoming too complex to control. There are four steps to design an acceptable model of System Identification:

- Perform experiments, and collect sampling data.
- Determine/choose model structure.
- Estimate model parameters.
- Model validation.

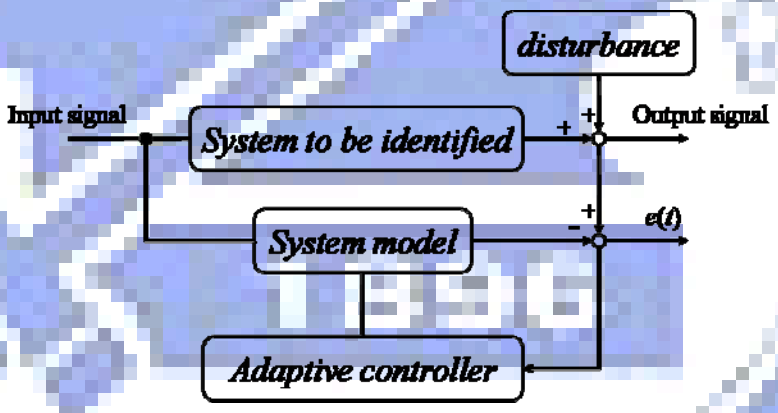

Fig. 3.8 system identification

Input signal: The input signal is used in a system identification experiment. It has a significant influence on the resulting parameter estimates. Sometimes, the input signal must be introduced to yield a reasonable identification results. There are three input signals can used in the system identification in the identification experiment:

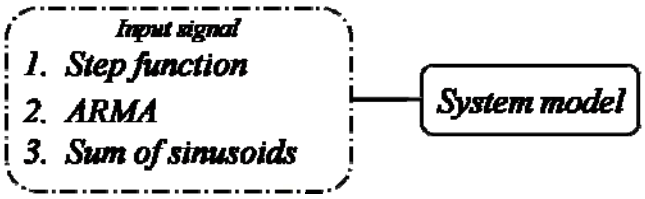

Fig. 3.9 input signals

1. Step function:

A step function is given in:

$$u(t)=\begin{cases}0 & t<0\\ u_0 & t\geq 0\end{cases}$$

The step input signal gives information about the dynamics. Rise time, sitting time, overshoot and static gain are directly related to the frequency response.

2. Autoregressive moving average process (ARMA):

$$C(z^{-1})u(t)=D(z^{-1})\cdot e(t)$$

$$C(z^{-1})=1+c_1\cdot z^{-1}+\ldots+c_{mc}\cdot z^{-mc}$$

$$D(z^{-1})=1+d_1\cdot z^{-1}+\ldots+d_{md}\cdot z^{-md}$$

Different parameters C_n and D_n lead to input signal emphasizing the identification in different frequency ranges.

3. Sum of sinusoids:

$$u(t)=\sum_{j=1}^{m}a_j\cdot\sin(\omega_j\cdot t+\theta_j)$$

$$0\leq\omega_1\leq\omega_2\leq\omega_3\leq\omega_4\leq\ldots\leq\pi$$

It can choose the parameter of the a_j, ω_j, and θ_j.

3.5 Least squares method

Least squares method is the best method of the system identification to make a feasible model. The simplest parametric model is linear regression. It can be shown

in:

$$y(t) = \hat{y}(t) + e(t) = \phi^T(t) \cdot \theta + e(t) \tag{29}$$

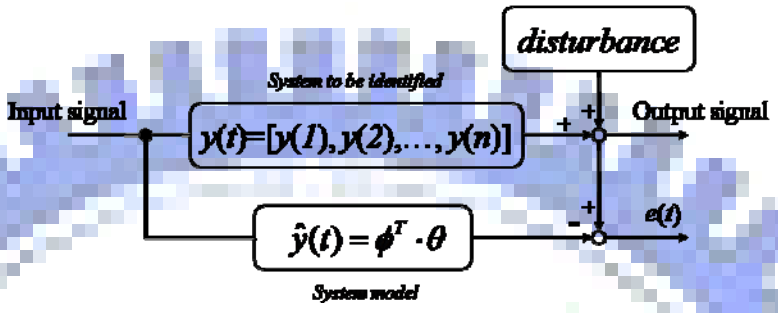

Fig. 3.10 parametric model

The data $y(t)$ is the values of system measurement. $\phi(t)$ is the known values, and θ is a vector of unknown parameters. Given an input signal, the method wants to calculate the unknown parameter θ. The way is to minimize the modeling errors $e(t)$ that between the actual $y(t)$ and the model prediction $y(t)$. The system identification model must be more similar than the actual system.

The actual output signal y includes:

$$y = \left[y(1), y(2), y(3), ..., y(n) \right]^T \tag{30}$$

Suppose that input signals and output signals are in discrete time t. The sample values can be related through a linear difference equation.

$$y(t) + a_1 \cdot y(t-1) + a_2 \cdot y(t-2) + a_3 \cdot y(t-3) + ... + a_n \cdot y(t-n)$$

$$= b_1 \cdot u(t-1) + b_1 \cdot u(t-2) + ... + b_m \cdot u(t-m) + v(t) \tag{31}$$

The disturbance $v(t)$ is described as a moving average (MA) of a noise sequence $e(t)$, and the n steps and m steps are the phase shift in the dynamic system.

$$y(t) = \phi^T(t) \cdot \theta + v(t) \tag{32}$$

$$\theta = [a_1, a_2, ...a_n, b_1, b_2, ...b_m]^T$$

a_n and b_n are the unknown dynamical parameters.

$$\phi^T = [-y(t-1), -y(t-2), ..., -y(t-n), u(t), u(t-1), u(t-2), ..., u(t-m)]$$

$$v(t) = C(z^{-1}) \cdot e(t) \tag{33}$$

$$C(z^{-1}) = 1 + c_1 \cdot z^{-1} + c_2 \cdot z^{-2} + c_3 \cdot z^{-3} + c_4 \cdot z^{-4} + ... + c_p \cdot z^{-p}$$

3.6 ARMAX model

The ARMAX model includes an autoregressive (AR) part, a moving average (MA) errors part, and a control unknown part.

The ARMAX model is referring Eq.32 and Eq.33 to:

$$\underbrace{A(z^{-1}) \cdot y(t)}_{autoregressive\ \text{part}} = \underbrace{B(z^{-1}) \cdot u(t)}_{control\ \text{part}} + \underbrace{C(z^{-1}) \cdot e(t)}_{moving\ averagep\ \text{part}}$$

The function can use actual sampling output signal $y(t)$ and an ideal output signal $y(t)$ that is expected by the ideal model.

$$e(t) = y(t) - \hat{y}(t) \tag{34}$$

$$e(t) = y(t) - \hat{y}(t) = y(t) - \phi^T(t) \cdot \theta$$

The Least squares method uses the sum of squared errors (SSE).

$$\sum_{t=1}^{N} e^2(t) = e^T \cdot e \tag{35}$$

$$SSE = e^T \cdot e = y^T \cdot y + \theta^T \cdot \phi^T \cdot \phi \cdot \theta - 2 \cdot \theta^T \cdot \phi^T \cdot y \tag{36}$$

The unknown model vector θ will gain and that the disturbance $e(t)$ that between these two vectors must to be the minimum. In this case, the SSE is minimized and approach to zero.

$$y(t) = \hat{y}(t) + e(t) = \phi^T(t) \cdot \theta + \underbrace{e(t)}_{\approx 0} = \phi^T(t) \cdot \theta \tag{37}$$

$$\frac{\partial(SSE)}{\partial \theta} = \frac{\partial\left(e^T \cdot e\right)}{\partial \theta} \quad -2 \cdot \phi^T \cdot y + 2 \cdot \phi^T \cdot \phi \cdot \theta = -2 \cdot \phi^T \cdot \left(y - \phi \cdot \theta\right) \approx 0 \tag{38}$$

The last term $y - \phi \cdot \theta$ contains unknown value. The SSE is minimal when the

last term is the minimum. The solution of least squares parameter estimate is

$$\hat{\theta} = \left(\phi^T \cdot \phi\right)^{-1} \cdot \phi^T \cdot y \tag{39}$$

Assume further Eq.36 that $e(t)$ is a noise or disturbance and the estimate $\hat{\theta} = \left(\phi^T \cdot \phi\right)^{-1} \cdot \phi^T \cdot y$. There are two properties hold:

$$1:\ E\left(\hat{\theta}\right) = E\left[\left(\phi^T \cdot \phi\right)^{-1} \cdot \phi^T \cdot y\right] = E\left[\left(\phi^T \cdot \phi\right)^{-1} \cdot \phi^T \cdot \left(\phi \cdot \theta + e\right)\right]$$

$$= \theta + \left(\phi^T \cdot \phi\right)^{-1} \cdot \phi^T \cdot E(e) = \theta$$

$\hat{\theta}$ is an unbiased estimate of θ.

$$2:\ E\left[\left(\hat{\theta} - \theta\right)\left(\hat{\theta} - \theta\right)^T\right] = E\left\{\left[\left(\phi^T \phi\right)^{-1} \cdot \phi^T \cdot E(e)\right] \cdot \left[\left(\phi^T \phi\right)^{-1} \cdot \phi^T \cdot E(e)\right]^T\right\}$$

$$= \left(\phi^T \cdot \phi\right)^{-1} \cdot \phi^T \cdot E(e \cdot e^T) \cdot \phi \cdot \left(\phi^T \cdot \phi\right)^{-1}$$

Because that the noise is used to $E(e \cdot e^T) = CI$, so the covariance matrix of $\hat{\theta}$ is shown as $\operatorname{cov}(\hat{\theta}) = C\left(\phi^T \cdot \phi\right)^{-1}$.

$$\operatorname{cov}\left(\hat{\theta}\right) = \frac{C}{N} \cdot \left(\frac{\phi^T \cdot \phi}{N}\right)^{-1} \to 0 \qquad N \to \infty \text{ in the finite full rank matrix.}$$

It introduces a symbol (n) to represent the fact that n sampling data points.

$$\hat{\theta}(n) = \left[\phi^T(n) \cdot \phi(n)\right]^{-1} \cdot \phi^T(n) \cdot y(n) = \frac{1}{n} \cdot \sum_{t=1}^{n} y(t) \tag{40}$$

$$\hat{\theta}(n) = \frac{1}{n} \cdot \sum_{t=1}^{n} y(t) = \frac{1}{n} \cdot \left(\sum_{t=1}^{n-1} y(t) + y(n)\right) = \frac{1}{n} \cdot \left[(n-1) \cdot \hat{\theta}(n-1) + y(n)\right]$$

$$= \frac{1}{n}\left[n \cdot \hat{\theta}(n-1) - \hat{\theta}(n-1) + y(n)\right] = \hat{\theta}(n-1) - \frac{1}{n} \cdot \left[y(n) - \hat{\theta}(n-1)\right]$$

$$\Rightarrow \hat{\theta}(n) = \hat{\theta}(n-1) + K(n) \cdot e(n) \tag{41}$$

$\hat{\theta}(n)$: the estimation of the model parameters in the sampling time n

$e(n)$: the errors between the measured output signal $y(n)$ and the model output signal.

$K(n)$: a weighting factor should be shown how much the value of $e(n)$ will modify the parameter vector.

Suppose at sampling time (n), we already calculated $\hat{\theta}$, but the new output signal $y(t)$ is available at time ($n+1$), we need to recalculate $\hat{\theta}$.

$$\hat{\theta}(n+1) = \hat{\theta}(n) + correction\ \ factor \tag{42}$$

When the sampling time n is the same as the new sampling data time $n+1$, the ideal model is the optimum solution that the correction factor would be close to zero. It can be computationally more efficient and less memory intensive, especially if the system can avoid doing large matrix inverse calculations. It gives an estimate of the model from the first step and implements the real-time responses of the system. In the following we will derive the recursive form of the least squares algorithm by modifying the non-continuous sampling data. So, the model parameter vector is computed.

$$\phi(n)^T \cdot y(n) = \phi(n-1)^T \cdot y(n-1) + \phi(n) \cdot y(n) \tag{43}$$

$$P^{-1}(n) = \phi(n)^T \cdot \phi(n) = \sum_{t=1}^{n} \phi(t) \cdot \phi(t)^T = \sum_{t=1}^{n-1} \phi(t) \cdot \phi(t)^T + \phi(n) \cdot \phi(n)^T$$
$$= P^{-1}(n-1) + \phi(n) \cdot \phi(n)^T \tag{44}$$

$$\hat{\theta}(n) = \left[\phi(n)^T \cdot \phi(n)\right]^{-1} \cdot \phi(n)^T \cdot y(n) = P(n) \cdot \left[\phi(n-1)^T \cdot y(n-1) + \phi(n) \cdot y(n)\right]$$
$$= \hat{\theta}(n-1) + \left[P(n) \cdot \phi(n)\right] \cdot \left[y(n) - \phi(n)^T \cdot \phi(n-1)^T\right] \tag{45}$$

$$\hat{\theta}(n) = \hat{\theta}(n-1) + K(n) \cdot \varepsilon(n) \tag{46}$$

$$P(n) = \left[P^{-1}(n-1) + \phi(n) \cdot \phi(n)^T\right]^{-1} = P(n-1) - \frac{P(n-1) \cdot \phi(n) \cdot \phi^T(n) \cdot P(n-1)}{1 + \phi^T(n) \cdot P(n-1) \cdot \phi(n)}$$

The linear function $y(t) = \phi^T(t) \cdot \theta + e(t)$ to be minimized in a least squares algorithm $y = \sum_{t=1}^{n} \left[e(t)\right]^2$ is:

$$V(\theta)=\sum_{t=1}^{n}\left[y(t)-\phi^{T}(t)\cdot\theta\right]^{2}=\sum_{t=1}^{n}\lambda^{n-t}\left[y(t)-\phi^{T}(t)\cdot\theta\right]^{2} \tag{47}$$

When the $\lambda<1$, it is supposed to *0.99* or *0.95*. The forgetting factor is useful in the linear system model. The forgetting factor makes that the order data has less effect in the coefficient estimation. This meaning that the measurements obtained previously are discounted. Real Time Identification is using the RLS algorithm with a forgetting factor λ. The properties of the process may change very slowly with time, and the algorithm is able to track the time-varying parameters. The smaller the value of forgetting factor, the quicker the information in previous data will be forgotten.

$$\lambda=1$$

$$P(n)=\frac{1}{\lambda}\cdot\left[P(n-1)-\frac{P(n-1)\cdot\phi(n)\cdot\phi^{T}(n)\cdot P(n-1)}{1+\phi^{T}(n)\cdot P(n-1)\cdot\phi(n)}\right] \tag{48}$$

The RLS algorithm is given by:

$$\phi(n)=\left[-y(n-1),u(n-1),e(n-1)\right]^{T}$$

$$e(n)=y(n)-\phi^{T}(n)\cdot\hat{\theta}(n-1)$$

$$P(n)=\frac{1}{\lambda}\cdot\left[P(n-1)-\frac{P(n-1)\cdot\phi(n)\cdot\phi^{T}(n)\cdot P(n-1)}{1+\phi^{T}(n)\cdot P(n-1)\cdot\phi(n)}\right]$$

$$K(n)=P(n)\cdot\phi(n)$$

$$\hat{\theta}(n)=\hat{\theta}(n-1)+K(n)\cdot e(n) \tag{49}$$

It has four steps to determining the ARMAX structure in the RLS algorithm:

$$A(q^{-1})\cdot y(t)=B(q^{-1})\cdot u(t)+C(q^{-1})\cdot e(t)$$

$$y(t)=-a_1\cdot y(t-1)-a_2\cdot y(t-2)-\ldots-a_{na}\cdot y(t-n_a)+b_1\cdot u(t-1)$$

$$+b_2\cdot u(t-2)+\ldots+b_{nb}\cdot u(t-n_b)+c_1\cdot e(t-1)+c_2\cdot e(t-2)+\ldots$$

$$+c_{nc}\cdot e(t-n_c)+e(t)$$

1. Initialization:

   Set $\hat{\theta}(0)$, $P(0)$, $e(0),\ldots,e(1-n_c)=0$, and the model starts from *t+1*

2. It will measure current sampling output data at the time $t=n$.

3. It uses RLS method to $e(n)$, $\hat{\theta}(n)$, and $P(n)$.

4. $\hat{\theta}(n)\rightarrow\hat{\theta}(n-1)$, $P(n)\rightarrow P(n-1)$ and $e(n)\rightarrow e(n-1)$ to the next step *t=n+1*,But it considers in the linear system by:

   $$y(t)=\phi^T(t)\cdot\theta+e(t)$$

IV. TWO DEGREE OF FREEDOM IN DUAL-STAGE SERVO SYSTEM

4.1 dual-stage control loop

Industries are striving for ODDs with smaller form factors and higher recording density. Conventionally, the VCM is used as the sole actuator in ODDs. With the amazing increment of focus speed, VCM cannot support the position accuracy for the narrower track width, because the limited bandwidth of VCM may not allow the servo loop to sufficiently suppress the high-frequency disturbance. A high-track density requires a higher precision servo system, which cannot be achieved by the ODDs employing the sole actuator VCM. Therefore, the seesaw actuator has the angle of inclination in horizontal plane when the motion of focusing the disk. The angle of the unnecessary inaccuracy causes the VCM actuator not to focus in a precise pitch. The servo mechanism of dual-stage micro actuator PZT, which holding the optical read/write head may be embedded in the arm of the seesaw suspension is placed in front of seesaw swing-arm. This secondary micro-actuator is made of piezo-electronic material (PZT-5Z) [4]. Although the displacement of the PZT actuator is smaller than the major (seesaw) actuator, the suspension produces a tilt to the horizontal plane when the optical head focuses the optic axis of disc. The PZT actuator can be effectively decrease the focusing time and correct the departure. It has been proposed to perform the fine positioning for ultra-high focusing speed. In view of the control point, it designs appropriate VCM and micro-actuator PZT controllers. A micro-actuator controller has been proposed as an effective way to attain the sufficiently high servo bandwidth and suppress the high-frequency noise, but the piezo-effect produces the new periodic disturbance.

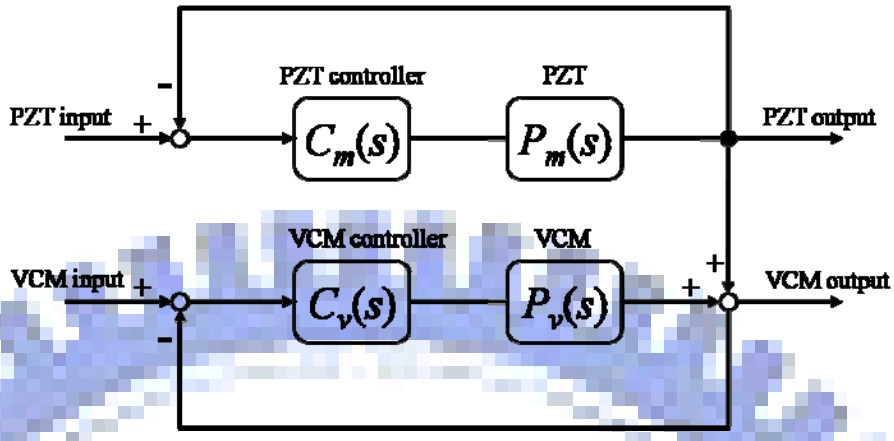

Fig. 4.1 Two-input-two-output control

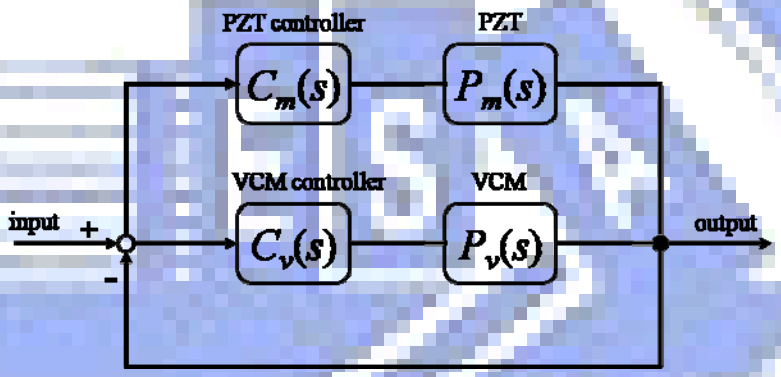

Fig. 4.2 Two-input-one-output control

In accordance with mechanical requirement, dual-stage servo system is generally designed as two typical configurations. The first one is a two input two output control system and the second one is a two input one output control system. The signal inputs in micro-actuator and major VCM and controller responds to signals from VCM and PZT output singly or position error signal (PES) both PZT and VCM. The PES observed the robustness of the dynamic system such as high frequency disturbances and non-linear uncertain variations.

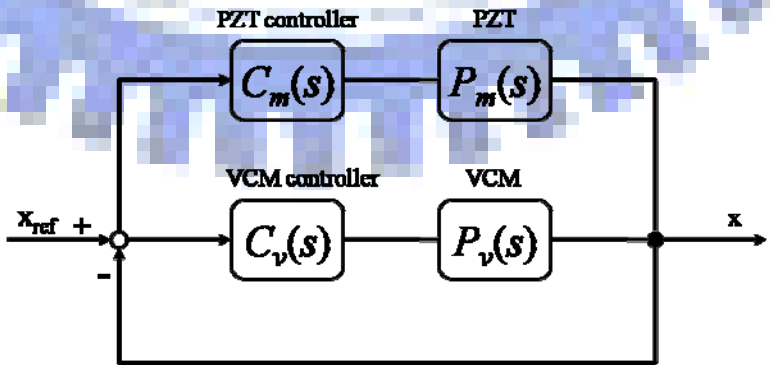

Fig. 4.3 dual-stage control loop

The more control emphasis is placed on the micro actuator than the VCM. This configuration constructs the PZT actuator to predict the displacement signal of the VCM controller at the same time. It can obtain decoupling of the two actuator loops. The dual stage control loop has better disturbance rejection capabilities than the VCM control loop. The dual stage control loop decouple should adhere to the guidelines so that the actuators will not conflict with each other's control action.

The open loop form the input x_{ref} to the output x is:

$$C_v(s)\cdot P_v(s)+C_m(s)\cdot P_m(s) \tag{50}$$

- 1. PZT control loop is: $C_m(s)\cdot P_m(s)$
- 2. VCM control loop is: $C_v(s)\cdot P_v(s)$

The feedback transfer function should be writing as;

$$\frac{x_{ref}}{x}=\frac{C_v(s)\cdot P_v(s)+C_m(s)\cdot P_m(s)}{1+C_m(s)\cdot P_m(s)+C_v(s)\cdot P_v(s)} \tag{51}$$

The sensitivity function of the dual stage loop is:

$$S(s)=\frac{1}{1+C_m(s)\cdot P_m(s)+C_v\cdot P_v(s)} \tag{52}$$

The decouple item will ensure that the VCM action in the low frequency and PZT action in the high frequency cooperate to reduce the outside disturbance within the servo bandwidth The PZT controller is designing by adjusting the system's high-frequency disturbances. The error rejection functions obtain from these two functions and indicate the input disturbance can be suppressed and constrain.

4.2 two degree of freedom control

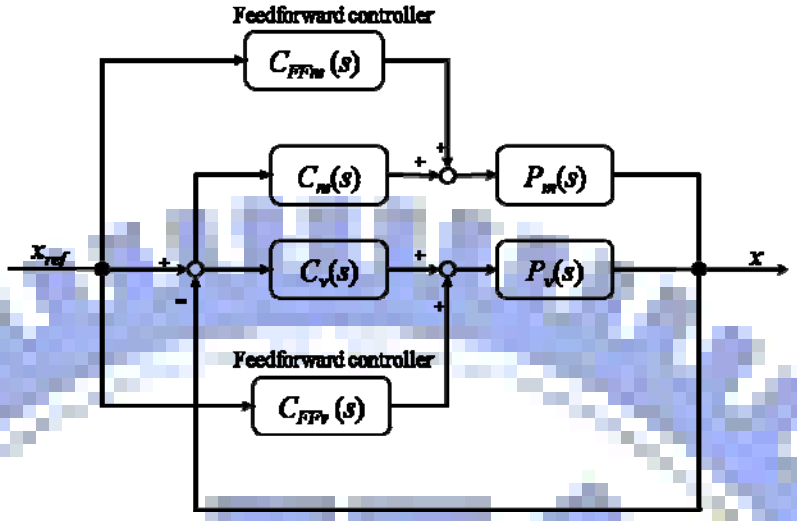

Fig. 4.4 two degree of freedom control

Referring Fig.4.4, the proposed feed-forward controller of DOF control can satisfy transient response specifications and maintain the tracking error within a tolerable limit for the uncertain track-following system. The robust feedback compensator defines both the frequency response from the disturbance to the output. The feed-forward compensator "$C_{FFv}(s)$ and $C_{FFm}(s)$" defines the frequency response from the reference input to the output. It is obvious that the feed-forward compensator is not able to improve the stability of the feedback closed-loop. The feedback controller must be designed to stabilize the servo system.

The closed loop transfer function form the input signal x_{ref} to the head displacement signal x is expressed as:

$$\frac{x_{ref}}{x} = \frac{C_{FFv}(s)\cdot P_v(s) + C_v(s)\cdot P_v(s) + C_{FFm}(s)\cdot P_m(s) + C_m(s)\cdot P_m(s)}{1 + C_v(s)\cdot P_v(s) + C_m(s)\cdot P_m(s)} \quad (50)$$

Referring the Eq.50 and Eq.51, to determine the stability of the dual actuator system when the PZT actuator is not activated, the seesaw feedback loop must be stable by itself. The major controller designs by the basic performance. Therefore, it uses the open loop function to attain the stable phase margin and gain margin. The relative effect is conspicuous in the low frequency range and slight in the high

frequency range. The PZT controller is designing by adjusting the seesaw's outside disturbances, and shows the proposed actuator controller which has two following algorithms [3]:

1. The track-following system design for ODDs is to construct the system with better performance and robustness against modeling uncertainties and various disturbances.
2. The robust control problem deals with finding feedback robust controller that guarantees robust stability of the closed loop and controlled outputs being less than a given bound.

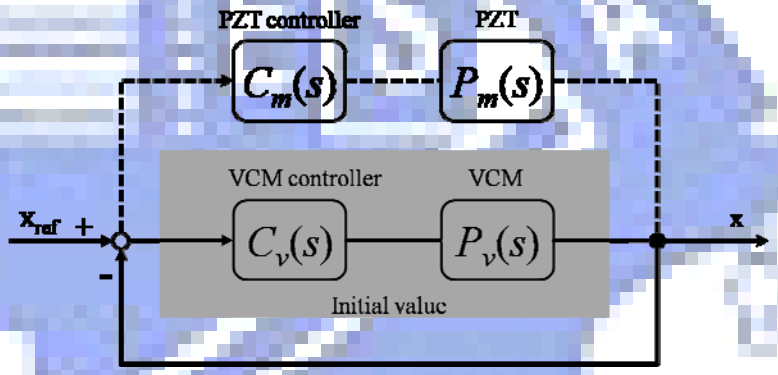

Fig. 4.5 action in initial time

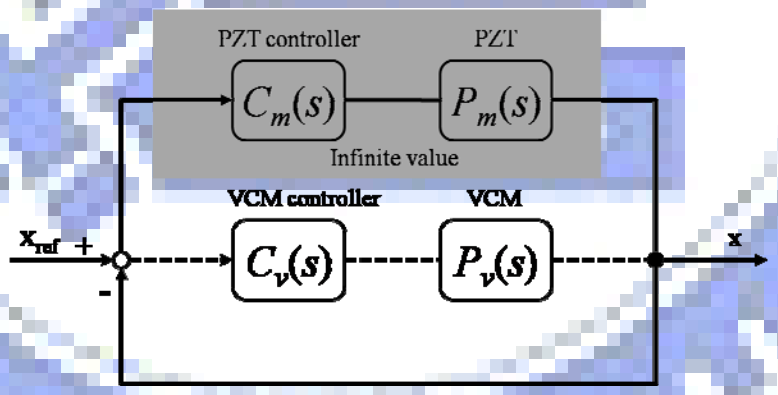

Fig. 4.6 action in infinite time

The open control loop approaches to the VCM actuator working alone in the low frequency. It will be ignored the action of the PZT actuator in the initial value. $C_v(s)$ can be designed to stabilize by:

$$\left|C_m(s)\cdot P_m(s)+C_v(s)\cdot P_v(s)\right|\approx\left|C_v(s)\cdot P_v(s)\ \right| \qquad (s\to 0) \tag{51}$$

Referring to the Eq.51, the two input one output system can be made to converge to this parallel loop. The major controller designs by the basic performance to determine the system stability when the PZT actuator doesn't work, the VCM actuator must be stable by itself. The VCM controller $C_v(s)$ is designed to stabilize in the low frequency. Based on these constraints and the assumption that the bandwidth of the micro actuator PZT is higher than that of the VCM (which is a reasonable one in the application of PZT micro actuator in seesaw ODDs), the frequency of overall bandwidth s is also much higher than PZT. When the PZT actuator almost works in the high frequency alone, it makes the VCM open control loop $\left[C_v(s)\cdot P_v(s)\right]$ to approximate zero. It will be ignored the action of the VCM actuator in infinite. $C_m(s)$ can be designed to stabilize by:

$$C_m(s)\cdot P_m(s)+C_v(s)\cdot P_v(s)\xrightarrow[(s\to\infty)]{}C_m(s)\cdot P_m(s) \tag{52}$$

V. HIGH SPEED PERIODIC DISTURBANCE REJECTION USING ZPET-FF CONTROL

5.1 ZPET-FF loop

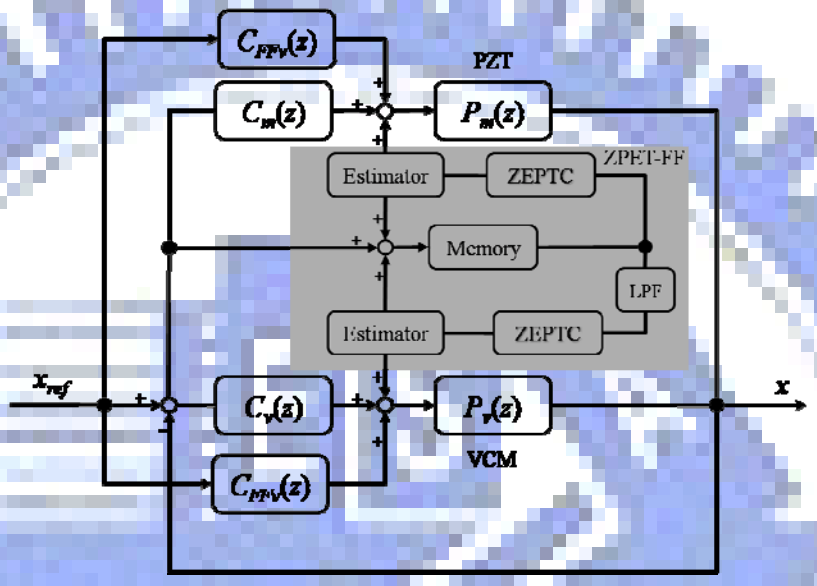

Fig. 5.1 ZPET-FF controller model

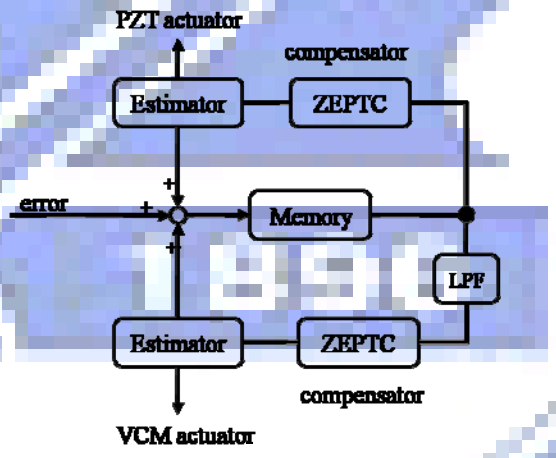

Fig. 5.2 ZPET-FF loop

In the optical disk recording system, the focusing servo system must have a precise focusing response whose error is less than *0.1*[μm] for a reference input signal with an amplitude of *100*[μm]. Essentially, the desired position reference of the focusing servo system is zero. However, the focusing servo system for optical disk always has the position disturbance input**.** The maximum amplitude of the

position disturbance input is about $100[\mu m]$ peak-to-peak. Therefore, it is often difficult for only the robust feedback control to follow the track to keep the residual focusing error below the tolerance of 100 $[\mu m]$ peak-to-peak.

For suppressing the periodic disturbance, this paper proposes a new robust feed-forward focusing servo system based on both "zero phase error tracking" (ZPET) control system and disturbance observer for an optical disk recording system [6] [7]. The new configuration of the ZPET control loop is shown in the Fig5.1 and Fig5.2. This compensator ZPETC reduces the periodic disturbances caused by piezoelectric effect. It ignored the ZPET-FF loop, and the closed loop is expressed as:

$G_{closed}(z)$:

$$\frac{C_{FFv}(z)\cdot P_v(z)+C_v(z)\cdot P_v(z)+C_{FFm}(z)\cdot P_m(z)+C_m(z)\cdot P_m(z)}{1+C_v(z)\cdot P_v(z)+C_m(z)\cdot P_m(z)} \tag{53}$$

5.2 Estimators of VCM and PZT

However, the ordinary optical disk recording system can't get the position reference input signal. Because it is detecting signal is only a focusing error. In order to overcome this problem, it proposes a new estimation method of position reference input signal for the pre-compensator of feed-forward controller. The ZPETC and estimator are expressed as:

$$Estimator_{vcm}=\frac{C_{FFv}(z)\cdot P_v(z)+C_v(z)\cdot P_v(z)}{1+C_v(z)\cdot P_v(z)+C_m(z)\cdot P_m(z)} \tag{54}$$

$$Estimator_{PZT}=\frac{C_{FFm}(z)\cdot P_m(z)+C_m(z)\cdot P_m(z)}{1+C_v(z)\cdot P_v(z)+C_m(z)\cdot P_m(z)} \tag{55}$$

Hence, using the memory, the proposed estimation method obtains the input variable $t+2$ of the pre-compensator, which is-the two sampling forward. The proposed method estimates the position reference input signal by using the focusing error. Generally, as the high speed focusing servo system does not move the actuator

in the very narrow space, this paper treats the position reference input signal as the periodic function. It proposes a new estimation method of the two sampling forward tracking error $e(t+2)$. This paper treats the focusing error $e(t)$ as a memory to obtain the two sampling forward error $e(t+2)$. The memory is used to memorize the focusing error of seesaw focusing quake. The system memory M step is to fit the actuator motion. The focusing errors give an $m=2$ step memories to pass the ZPETC block. In this system, the focusing error is learned repetitively using a memory, then the system rejects the amount of focusing error. The passing focusing errors compare to the next signal errors then reduced in the ZPET-FF loop. The difference between both feed-forward control loops is FF-PZT control loop without the LPF. Fig. 5.2 shows the valid repetitive control system added to a LPF in the VCM control loop. The LPF can effective restrain high-frequency disturbance to the VCM actuator.

VI. EXPERIMENT AND SIMULATION

6.1 Seesaw frequency response and PZT frequency response

Analyzing System is an important task of which it would like to control and affect the behavior. A model is the knowledge of the properties of a system. It is necessary to have a model of the system in order to solve problems of control and system design. In the experimental implementation, the LDV captures the overall displacement of the dual actuators. The Dynamic Signal Analyzer (DSA) performs the measurement of Seesaw and PZT models with the method of identification in frequency domain. The System Identification experiments are performed on the system. The step input signal data can give information about the dynamics characteristics. Rise time, overshoot and static gain are directly related to the step response of system. It has a significant influence on the resulting parameter estimates. Sometimes, the input signal must be introduced to yield a reasonable identification results. A model is fitted to the signal's data by assigning accepted values to the parameters of model. System identification is the field of modeling dynamic systems from experimental data of the LDV.

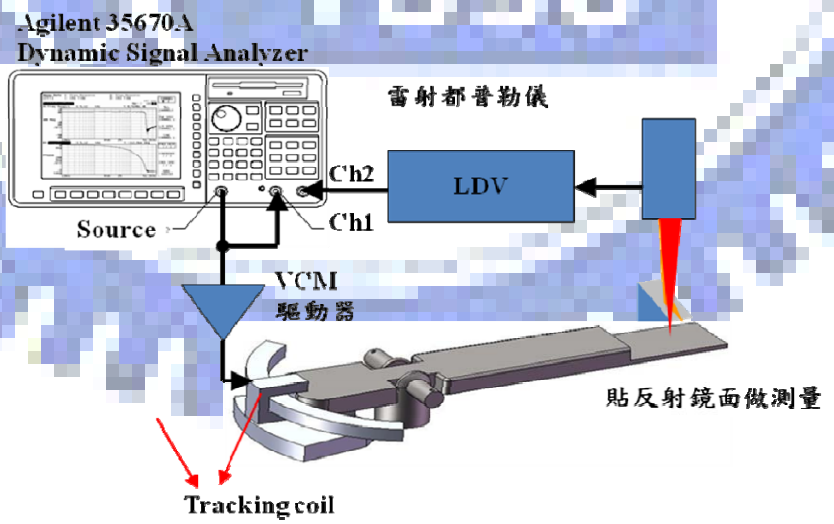

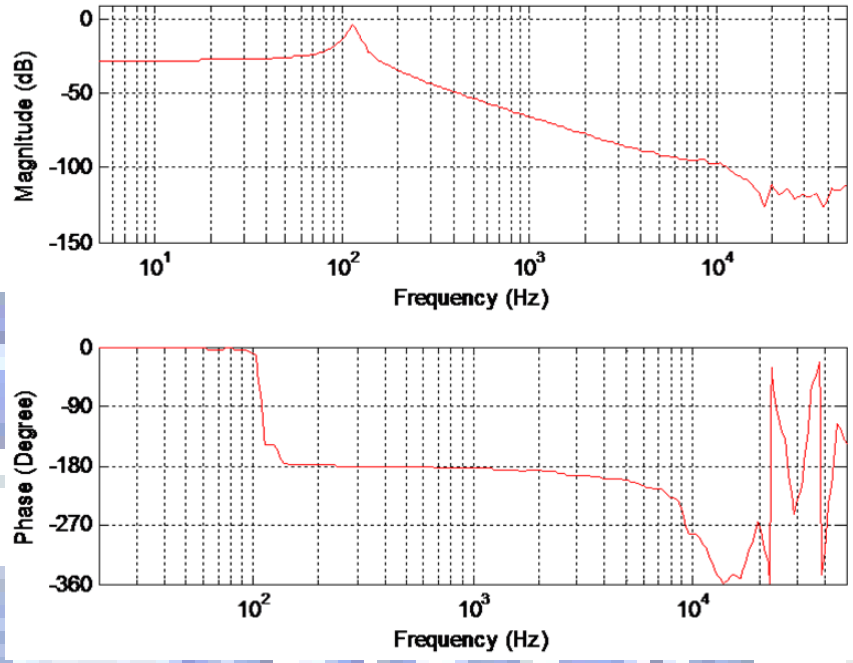

Fig. 6.1 Seesaw frequency response

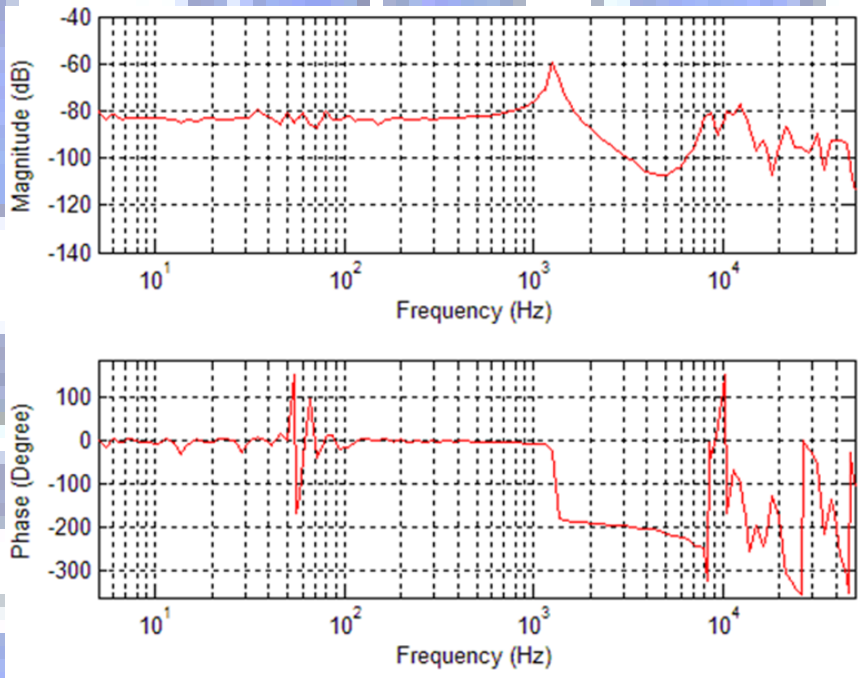

Fig. 6.2 PZT frequency response

特性專案	記號及單位	S-1	S-2	S-3	S-4	S-5	S-7	S-8	S-9	S-10	S-11	S-12 *
比誘電率	$\varepsilon^T/\varepsilon_0$	300	1050	2000	1400	1260	1580	1850	1350	1000	1300	1320
誘電損失	tg δ (%)	0.5	2.0	1.8	0.35	0.3	0.4	0.4	0.45	0.3	0.35	0.35
頻率定數	Np (Hz·M)		2020	1980	2050	2150	2270	2280	2250	2330	2235	2280
	Nt (Hz·M)	2245	2070	2050	2030	2100	2130	2150	2050	2100	2110	2080
共振頻率fr			2992	2933	3037	3185	3362	3377	3333	3451	3311	
耦合係數	Kt (%)	54	53	52	51	49	47	46	47	47	46	49
機械的Q	QM	55	80	76	400	900	1360	1450	1800	2000	1600	1000
等價壓電係數	d_{33}(x10 ^{12}M/V)		460	530	325	335	430	365	290	325	320	350
壓電出力係數	g_{33}(x10^{-3}V·M/N)		48.5	49.9	26.2	29.6	30.6	22	26.8	36.7	27.8	30.9
偏移量 代定電壓我用120v	nm		18.63	21.46	13.16	13.56	17.41	14.78	11.74	13.16	12.96	
密 度	P (x10^3 Kg/M^3)	7.2	7.55	7.56	7.7	7.75	7.76	7.78	7.85	7.84	7.9	7.8

Fig. 6.3 piezoelectric ceramic

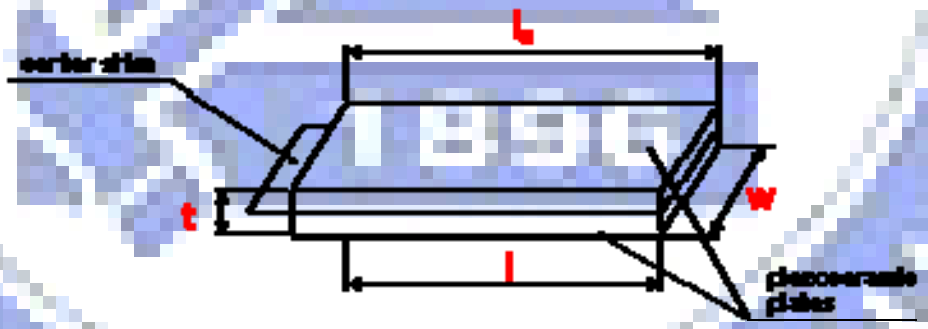

Fig.6.4 piezoelectric ceramic

6.2 piezoelectric ceramic

PZT(S-2):

Bimorph piezo-ceramic actuators are dedicated to replace electro-magnet actuators. Using the high efficient ceramics allows to meet the requirement of the control deflection and the control force. Their main advantages are low energy

consumption, higher control speed and small dimensions. S-2 is very high sensitivity material featuring extremely high permittivity, large coupling factor and piezoelectric constant. It has relatively low Currie temperature. This material is suitable for a wide range of high sensitivity applications with limited temperature range of operation.

thk=thickness

V=operating voltage

L=length

d_{31}*=piezoelectric coefficient*

N_1*=frequency constant*

$$\textit{vertical displacement } \Delta thk = \frac{3 \cdot d_{31} \cdot V \cdot L^2}{2 \cdot thk^2} \tag{60}$$

$$\Delta thk = \frac{3 \cdot \left(460 \times 10^{-12}\right) \cdot \left(120V\right) \cdot \left(15mm\right)^2}{2 \cdot \left(1mm\right)^2} = 18.63 \times 10^{-9} m = 18.63nm$$

$$\textit{resonant frequency } f_r = \frac{thk \cdot N_1}{3 \cdot L^2} \tag{61}$$

$$S\text{-}2 = \frac{\left(1mm\right) \cdot \left(2020\ Hz/m\right)}{3 \cdot \left(15mm\right)^2} = 2992.2592Hz$$

The measured frequency response is shown in Fig. 6.1 and Fig. 6.2, where the seesaw bandwidth is around *114.57* Hz with stable phase margin. The bandwidth of the plant is *114.57* Hz not enough to do a precise motion in the high frequency. The seesaw motion is perform a long focusing distance within *1000* Hz. The micro-actuator PZT works in the high frequency of *1000* Hz to *4000* Hz and has a short focusing distance of *15-18*nm. It decreases the focusing time and correct the optical departure usefully.

6.3 system identification

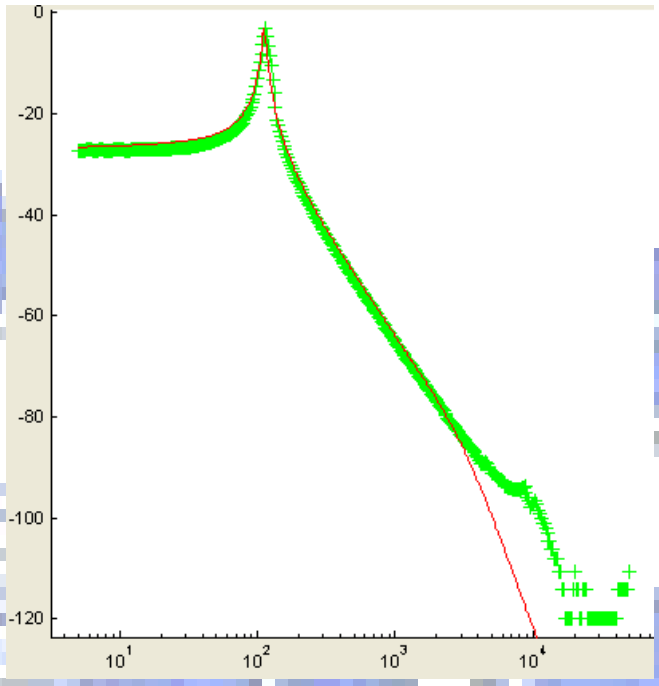

Fig. 6.5 System Identification of VCM

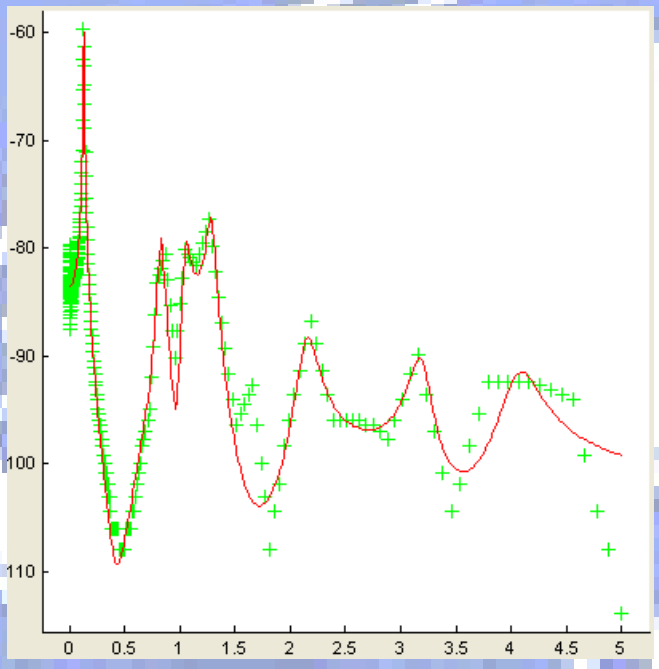

Fig. 6.6 System Identification of PZT

The VCM transfer function is:

$$\frac{9.159e\text{-}014s + 8.132e\text{-}012}{\begin{pmatrix}1.788e\text{-}048\,s^9 + 8.236e\text{-}044\,s^8 + 2.493e\text{-}037\,s^7 + 9.52e\text{-}033\,s^6 \\ +8.076e\text{-}027\,s^5 + 2.537e\text{-}022\,s^4 + 3.715e\text{-}018\,s^3 + 6.76e\text{-}016\,s^2 \\ +1.835e\text{-}012s + 1.766e\text{-}010\end{pmatrix}}$$

The PZT transfer function is:

$$\frac{\begin{pmatrix}9.87e\text{-}080s^{14} + 2.15e\text{-}075s^{13} + 1.24e\text{-}068\,s^{12} + 4.651e\text{-}064s^{11} + 5.459e\text{-}058s^{10} \\ +2.46e\text{-}053\,s^9 + 9.866e\text{-}048\,s^8 + 4.794e\text{-}043s^7 + 8.265e\text{-}038s^6 + 3.628e\text{-}033s^5 \\ +2.888e\text{-}028s^4 + 8.843e\text{-}024s^3 + 3.849e\text{-}019s^2 + 3.523e\text{-}015s + 1.97e\text{-}010\end{pmatrix}}{\begin{pmatrix}1.235e\text{-}074s^{14} + 6.026e\text{-}070s^{13} + 1.704e\text{-}063\,s^{12} + 5.648e\text{-}059s^{11} + 7.804e\text{-}053s^{10} \\ +1.622e\text{-}048s^9 + 1.449e\text{-}042s^8 + 1.71e\text{-}038s^7 + 1.145e\text{-}032s^6 + 7.346e\text{-}029s^5 \\ +3.902e\text{-}023s^4 + 1.222e\text{-}019s^3 + 4.767e\text{-}014s^2 + 2.868e\text{-}011s + 2.98e\text{-}006\end{pmatrix}}$$

The Least Squares method is the best method of the system identification. It can use a method that a sequence of model structures of increasing dimension to obtain the best fitted model within each of the model structures. Therefore, a better fit will be obtained with more free parameters in the high order model than in the sample order model. In determining the best model structure, the important thing is to investigate whether or not the improvement in the fit is significant. If a model is more complex than is necessary, the model may be over-parameterized. Therefore, the high order transfer function makes the feedback closed loop of the dual stage system very complex. To simplify the actuator's model is very important.

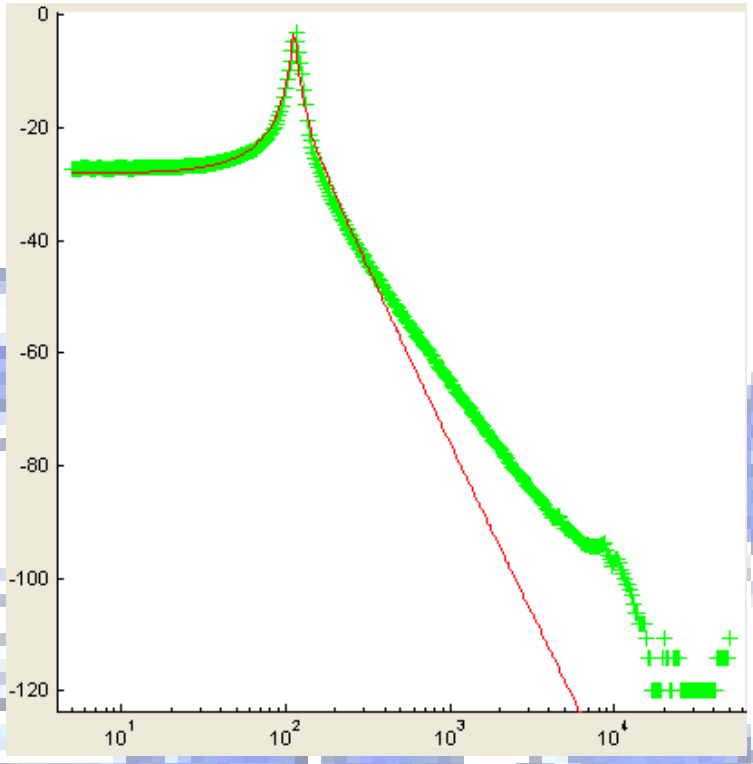

Fig. 6.7 System Identification of VCM

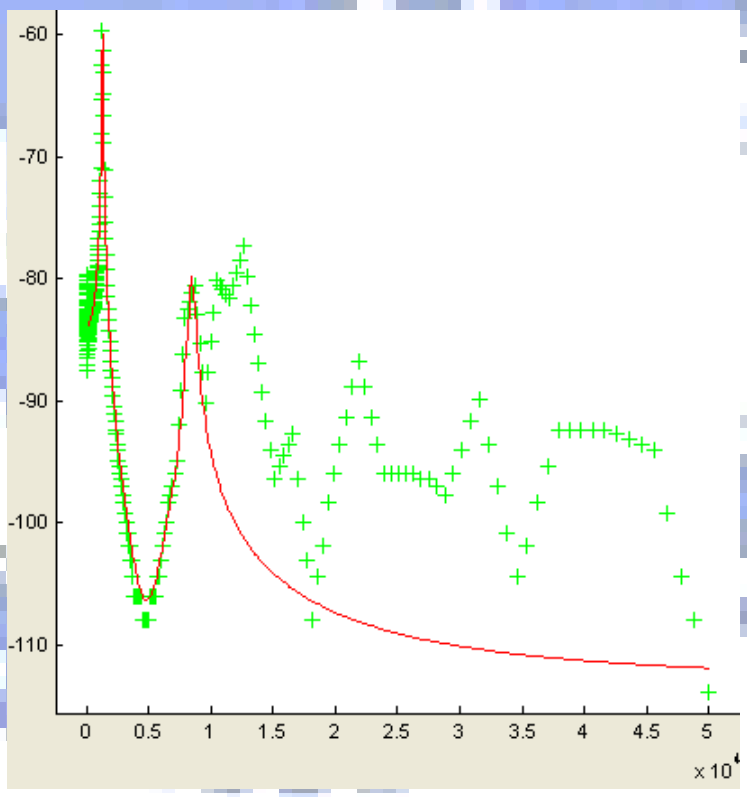

Fig. 6.8 System Identification of PZT

Fig. 6.7 and Fig. 6.8 shows the 4th order fitting curve, the red solid line is the estimated curve, and the green dashed one is the frequency response. By combining the frequency response and utilizing System Identification. The function of VCM and PZT are:

$$VCM: \frac{6.296e\text{-}014s + 4.288e\text{-}011}{\left(\begin{array}{c}1.642e\text{-}021s^4 + 2.645e\text{-}018s^3 + 3.165e\text{-}015s^2 + 1.385e\text{-}012s \\ + 1.09e\text{-}009\end{array}\right)}$$

$$PZT: \frac{\left(\begin{array}{c}3.585e\text{-}027\ s^4 + 6.445e\text{-}022s^3 + 1.334e\text{-}017s^2 \\ + 3.402e\text{-}013s + 1.937e\text{-}008\end{array}\right)}{\left(\begin{array}{c}1.63e\text{-}021s^4 + 6.053e\text{-}018s^3 + 4.709e\text{-}012s^2 \\ + 2.635e\text{-}009s + 0.0003038\end{array}\right)}$$

6.4 2DOF system response

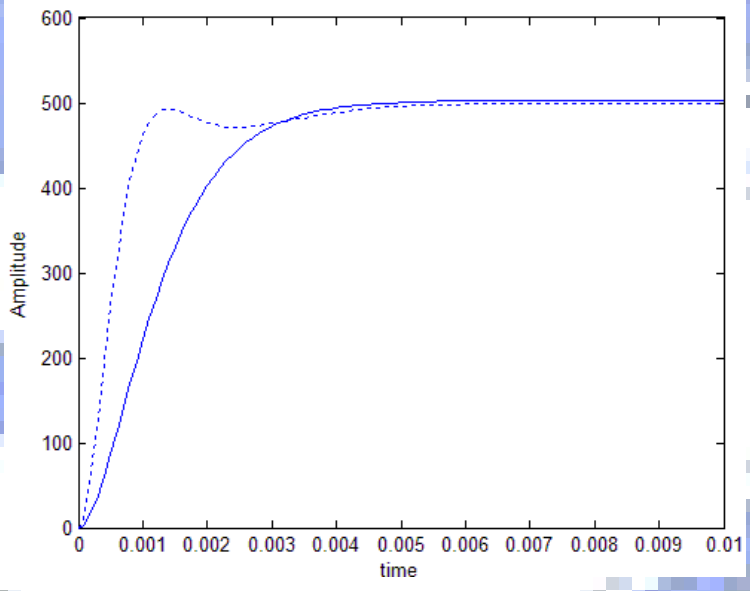

Fig. 6.9 servo system response

The 2DOF control loop demonstrates a larger bandwidth than the single feedback controller design. In time domain, the step responses of the servo system design is comparing in Fig. 6.9, the solid line is the 2DOF control loop, and the dash line is the feedback robust loop. Referring Fig. 6.9 the convergence speed of the two

degree of freedom design *0.0055* second is better than the conventional system *0.0062* second.

6.5 periodic disturbance response

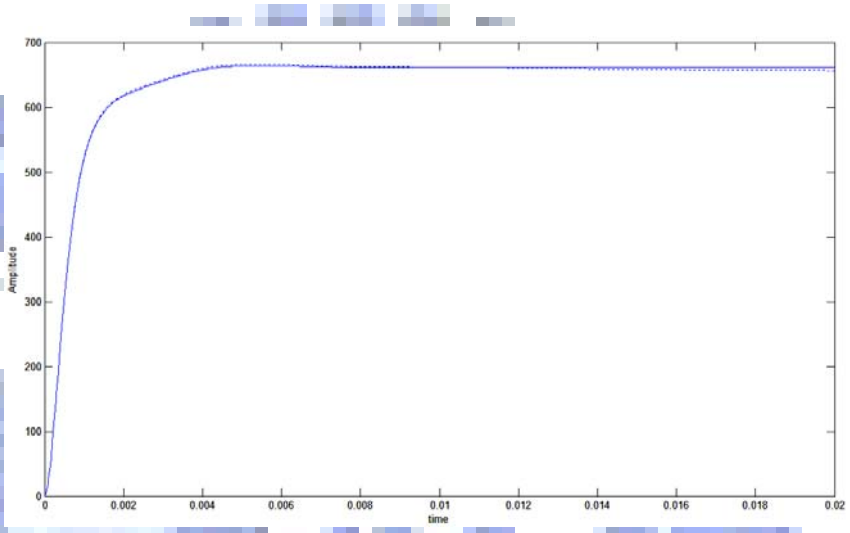

Fig. 6.10 periodic disturbance response

In the case of ZPET-FF control, although the servo system has the 10πperiod and 100 amplitude periodic disturbance, the residual focusing error signal is almost equal to zero at *0.007*second (solid line), and is better than the same scale of the FB control *0.011* second (dashed line). The settling time is faster than the conventional control in these simulation results. As the pre-compensator of ZPET-FF control compresses the focusing error using the anticipation value obtained from the estimated focusing error signal.

6.6 sudden disturbance reject

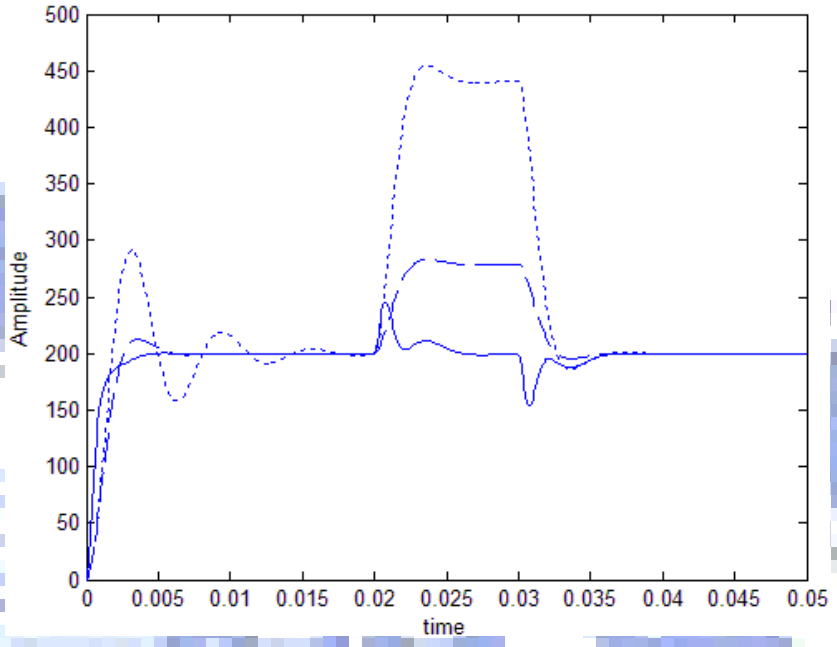

Fig. 6.11 sudden disturbance rejection

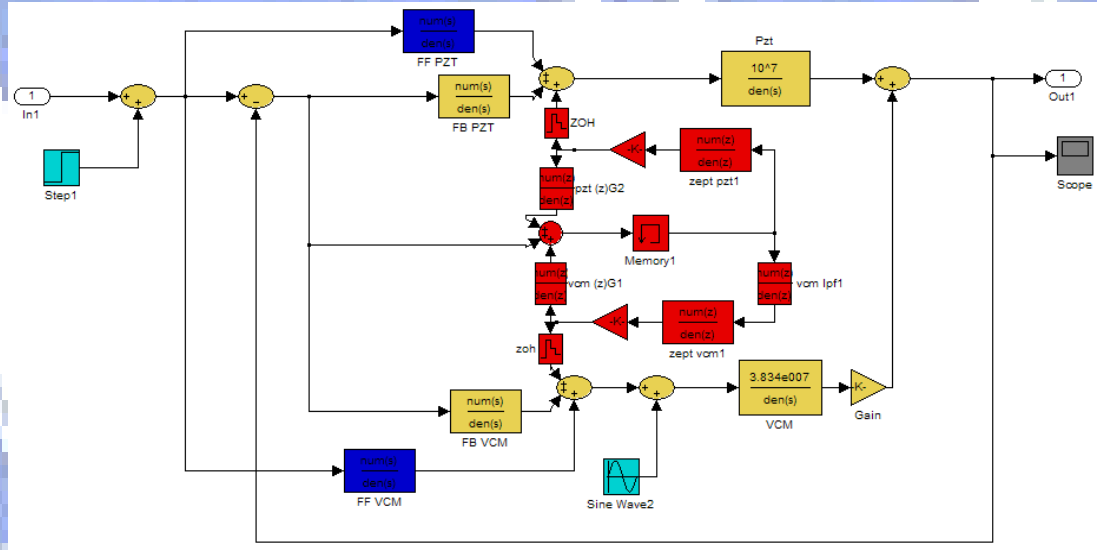

Fig. 6.12 control loop model

Fig. 6.11 and Fig. 6.12 shows the simulation results of the sudden disturbance (initial time *0.02* second and final time *0.03* second *100* amplitude step function in VCM actuator)for comparing the characteristics of the new control (solid line), robust control (dotted line), and conventional PID control (dashed line) at a dual stage servo system. Each control methods design to minimize the sudden disturbance.

In each compensator, the sudden disturbance of the new control is obvious within the tolerance level at this PZT focusing. The simulation results thus confirmed that the new control loop may allow precise control at very high speed focusing.

VI. CONCLUSION

ZPET-FF robust design in 2DOF of dual-stage system is proposed for high speed focusing in miniaturized ODD. The high-bandwidth micro-actuator working in the path can greatly improve the output response of reference focusing. The 2DOF construction of dual-stage actuator provides a fine focusing solution to overcome the signal actuator coarse motion. The feed-forward control signal should be injected to the VCM and PZT input in addition to the usual servo signal, which would guarantee that the primary actuator PZT can arrive the target eventually. This paper proposes a new robust focusing servo system for dual-stage mechanical system, which detects and suppresses the both periodic disturbance and sudden disturbance. The experimental results point out that the proposed sudden disturbance observer well estimate by robust controller. Moreover, in order to suppress the periodic disturbance, this paper designs the ZPET feed-forward servo system with prediction of focusing error. The experimental result confirms that the proposed robust tracking servo system reduces the focusing error and the influence of sudden disturbance.

Acknowledgment

Research supported by TDPA project 95-EC-17-A-07-S1-011, MOEA, Taiwan, ROC.

REFERENCES

[1]T. Hirano, L. S. Fan, W. Y. Lee, J. Hong, W. Imaino, S. Pattanaik, S. Chan, P. Webb, R. Horowitz, S. Aggarwal, and D. A. Horsley,“High-bandwidth high-accuracy rotary microactuators for magnetic hard disk drive tracking servos”, IEEE/ASME Trans. Mechatron., vol.3, pp. 156–165, Sept. 1998.

[2]R. B. Evans, J. S. Griesbach, andW. C. Messner, “Piezoelectric microactuator for dual stage control,” IEEE Trans. Magn., vol. 35, pp. 977–982, Mar. 1999.

[3]D. A. Horsley, D. Hernandez, R. Horowitz, A. K. Packard, and A. P.Pisano, “Closed-loop control of a micofabricated actuator for dual-stage hard disk drive servo systems,” in Proc. Amer. Control Conf., 1998, pp. 3028–3032.

[4]J. Ashley, M.-P. Bernal, G. W. Burr, H. Coufal, H. Guenther, J. A. Hoffnagle, C. M. Jefferson, B. Marcus, R. M. Macfarlane, and R. M. Shelby, “Holographic data storage,” IBM J. Res. Develop., vol. 44, pp. 341–368, 2000.

[5]T. Yamaguchi, H. Numasato, and H. Hirai, “A mode-switching control for motion control and its application to disk drives: Design on optimal mode-switching conditions,” IEEE/ASME Trans. Mechatron., vol. 3, pp. 202–209, Sept. 1998.

[6]Tomizuka, Y. 1987, " Zero Phase Error Tracking Algbrithm for Digital Control", ASME Journal of Dynamic systems, Measurement,and Control, Vol.109, PP. 65-68.

[7]Tomizuka, M. 1989, " Design of Digital Tracking Controllers for Manufacturing Applications", American Society of Mechanical Enginerrs. Xanufacturing Review Vo1.2, No. 2, pp. 134-141.

[8]Chia-Hsiang Heng, 1993, "Precision Tracking Control of Discrete Time Nonminimum-phase System", ASME. Journal of Dynamic System, Measurement, And Control, Vol. 115, pp. 238-245.

[9]Gross, Eric, Tomizuka, Mesayoshi and Messner Willian. March,1994, " Cancellation of Discrete Time Unstable Zeros by Feedforward Control", ASME, Journal of Dynamic System, Measurement and Control,

[10]Tung, E.D., 1993, " Feedforward Tracking Controller Design Based on the Identification Of Low Frequency Dynamics", ASME Journal of Dynamic Systems, Heasurement, And Control, Vol. 115, pp. 348-355.

[11]K.Ohishi, K.Kudo, K.Arai and H.Tokumaru, ”Robust High Speed Tracking Servo System for Optical Disk System”, Proc. of IEEE. 6th International Workshop on Advanced Motion Control, pp.92-97, 2000.

[12]K.Ohishi, K.Kudo, Y.Hayakawa, K.Arai, D.Koide and H.Tokumaru, ”Robust Feedforward Tracking Servo System for Optical Disk Recording System”, Proc. of IEEE. IECON’01,Vol.3, pp.1710-1715, 2001.

[13]K.Arai, H.Okumura, H.Tokumaru, and K.Ohishi : ”Improvement of Performance of a Tracking Servo System for an Optical Disk Drive”, Jpn. J. Appl. Phys.Vol.39, Part1, No.3B, pp.855-861,(2000)

[14]R. Nagamune, X. Huang, and R. Horowitz, “Multi-rate track-following control with robust stability for a dual-stage multi-sensing servo system in HDDs,” in Proc. Joint 44th IEEE Conf. Decision and Control and Eur. Control Conf., Seville, Spain, 2005, pp. 3886–3891

[15]D. Hernandez, S. Park, R. Horowitz, and A. Packard, “Dual-stage trackfollowing servo design for hard disk drives,” in Proc. American Control Conf., San Diego, CA, 1999, pp. 4116–4121.

[16]R. Nagamune, X. Huang, and R. Horowitz, “Robust control synthesis techniques for multirate and multi-sensing track-following servo systems in HDDs,” Computer Mechanics Lab., Univ. California, Berkeley,Tech. Rep., 2005.

[17]R. de Callafon, D. Harper, R. Skelton, and F. Talke, “Experimental modeling

and feedback control of a piezo-based milliactuator," J. Inform. Storage Process. Syst., vol. 1, no. 3, pp. 217–224, 1999.

[18] L. Fan, H. Ottesen, T. Reiley, and R. Wood, "Magnetic recording head positioning at very high track densities using a microaactuator-based, two-stage servo system," IEEE Trans. Ind. Electron., vol. 42, no. 3, pp. 222–223, Jun. 1995.

[19]D.Koide, H. Yanagisawa, H.Tokumaru, S. Nakamura, K.Ohishi, K.Inomata and T. Miyazaki: "High-speed Tracking Method using ZPET-FF Control for High-Data-Rate Optical Disk Drives", ISOM 2003 Technical Digest, pp.40-41, 2003.

[20]K.Arai, H.Okumura, H.Tokumaru, and K.Ohishi : "Improvement of Performance of a Tracking Servo System for an Optical Disk Drive", Jpn. J. Appl. Phys.Vol.39, Part1, No.3B, pp.855-861,(2000)

[21]Hsi-Fu Shih, Chi-Lone Chang, Kuei-Jen Lee, and Chi-Shen Chang: "Design of Optical Head With Holographic Optical Element for Small Form Factor Drive Systems" IEEE TRANSACTIONS ON MAGNETICS, VOL. 41, NO. 2, FEBRUARY 2005